

Determining the Fraction of Intrinsic C IV Absorption in Quasi-Stellar Object Absorption Line Systems

Gordon T. Richards¹ and Donald G. York²

Department of Astronomy and Astrophysics, University of Chicago, 5640 S. Ellis Avenue, Chicago, IL 60637

Brian Yanny and Ronald I. Kollgaard

Fermi National Accelerator Laboratory, Kirk Road and Pine Street, Batavia, IL 60510

S. A. Laurent-Muehleisen

UC-Davis and IGPP/LLNL, L-413, 7000 East Ave., Livermore, CA 94550

and

Daniel E. Vanden Berk

McDonald Observatory and Department of Astronomy, University of Texas at Austin, Austin, TX 78712

ABSTRACT

We present the results of an exhaustive study of QSO Absorption Line Systems (QSOALSs) with respect to intrinsic QSO properties using an updated catalog of data in the literature. We have searched the literature for 6 and 20 cm radio flux densities and have studied 20 cm contour plots from the Faint Images of the Radio Sky at Twenty centimeters (FIRST) VLA Survey in order to compare the absorption properties with radio luminosity, radio spectral index and radio morphology. Although the data in our catalog are decidedly heterogeneous, great care has been taken to account for potential biases during the course of our research. Analysis of relatively unbiased subcatalogs allows us to investigate the properties of QSOALSs with better statistics than with any single homogeneous catalog. This work focuses particularly on the nature of C IV QSOALSs and their distribution in velocity space in light of intrinsic QSO properties. We find that the distribution of narrow, C IV absorption systems with relative velocities exceeding 5000 km s^{-1} is dependent not only on the optical luminosity of the QSOs, but also on the radio luminosity, the radio spectral index and the radio morphology of the QSOs. These observations are apparently inconsistent with the hypothesis that these systems are predominantly due to intervening galaxies and it would seem that the contamination of the intervening systems (from 5000 to $75,000 \text{ km s}^{-1}$) by those that are intrinsic to the environment of the QSO is significantly larger than expected. We stress the need for truly homogeneous and unbiased surveys of QSOALS to confirm these results from our inhomogeneous data set.

Subject headings: gravitational lensing — quasars: absorption lines — quasars: general — radio continuum: galaxies

¹Also, Fermi National Accelerator Laboratory, Kirk Road and Pine Street, Batavia, IL 60510

²Also, Enrico Fermi Institute, 5640. S. Ellis Avenue, Chicago, IL 60637

1. Introduction

Although there was great debate (e.g., Bahcall & Salpeter 1966) over the origin of QSO absorption line systems for many years after they were first discovered (Burbidge, Lynds, & Burbidge 1966; Stockton & Lynds 1966), current interpretation treats systems with $v > 5000 \text{ km s}^{-1}$ as arising from intervening galaxies.³ Time and time again, observations have shown that narrow, C IV absorbers with velocities exceeding 5000 km s^{-1} are distributed in a way that is consistent with the absorbers being caused by intervening galaxies (Young, Sargent, & Boksenberg 1982; Sargent, Boksenberg, & Steidel 1988; Steidel 1990). It has also been shown that C IV absorption systems within 5000 km s^{-1} of the QSO are distinctly different from those at higher relative velocities and are probably intrinsic to the QSO environment; these are primarily strong systems and are biased towards steep-spectrum radio-loud objects (Foltz et al. 1986; Anderson et al. 1987; Foltz et al. 1988). Equally well accepted is that troughs, observed to at least $0.1c$, in the spectra of so-called Broad Absorption Line QSOs (BALQSOs) must be intrinsic to the QSO (Turnshek 1988). However, even though QSOs can clearly accelerate material to velocities exceeding 5000 km s^{-1} , few have argued that any significant fraction of the narrow, C IV lines blueward of 5000 km s^{-1} are related to the QSO.

In spite of the above statements, a search of the literature would turn up any number of examples of narrow, high ionization QSOALS that are intrinsic absorption candidates. Perry, Burbidge, & Burbidge (1978) present evidence that narrow, high velocity absorption lines may be intrinsic to OQ 172 and PHL 957 since their fine structure lines would seem to indicate very large electron densities. Weymann et al. (1979) discuss evidence for an ejected component of narrow absorption systems out to velocities of $18,000 \text{ km s}^{-1}$. Young et al. (1982) claim to see an excess of relatively narrow systems with $\beta < 0.1c$ in 3 QSOs. Even though these are BALQSOs, it establishes the possibility of *narrow*, high velocity systems. Foltz et al. (1986) find that the excess of associated absorption is dominated by strong systems and that there are 3 such systems in their sample with velocities greater than 5000 km s^{-1} . More recently, Borgeest & Mehler (1993) concluded that the “association hypothesis” was more probable than the “intervening hypothesis” for a large fraction of the C IV systems in 5 surveys of QSO absorption lines. Petitjean, Rauch, & Carswell (1994) have found super-solar abundances in 6 systems with $v < 13,000 \text{ km s}^{-1}$ and postulate that these systems are intrinsic. Arav, Li, & Begelman (1994) have modeled BALQSOs and find that the terminal velocity of radiatively accelerated clouds is on the order of $16,000$ to $25,000 \text{ km s}^{-1}$. Barlow, Hamann, & Sargent (1997) acknowledge the existence of narrow, intrinsic systems and give nine ways to tell the difference between a system that is intrinsic and one that is intervening. Jannuzi et al. (1996) describe a broad C IV absorber at $56,000 \text{ km s}^{-1}$ in PG 2302+039. Hamann et al. (1997) find evidence for relatively narrow, intrinsic absorption from 1500 to $51,000 \text{ km s}^{-1}$ in PG 0935+417, UM675 and Q2343+125.

In light of the above evidence, circumstantial as it may be, it should come as no surprise if it were found that a significant fraction of narrow C IV lines with high velocities turned out to be ejected material from QSOs rather than intervening galaxies. In this work we consider all C IV systems whose absorption redshifts are such that they are within $71,400 \text{ km s}^{-1}$ ($\beta = v/c = 0.238$), at which point C IV systems become blended with the Lyman α forest.

QSO absorption line systems may originate from any or all of 4 distinct environments including (1) the host galaxy of the QSO, (2) material ejected by the QSO, (3) the cluster environment of the QSO and

³Throughout this paper velocities (v) refer to the blueshifted velocity relative to the emission-line redshift of the QSOs, where $\beta (= v/c)$ is given by eq.(1) in §3.2.

(4) intervening galaxies along the line of sight. Throughout this paper we refer to any absorber that could be strongly affected by the radiation field of the QSO (which includes the first 3 classes listed above) as intrinsic. Note that this is in contrast to the definition that some have used in other work.

This body of work utilizes the QSO absorption line data collected by York et al. (1991), and began as a result of previous papers that draw upon the data from this catalog. Specifically, Vanden Berk et al. (1996) found that QSOs that have more C IV systems along their line of sight tend to be brighter than those that have fewer such systems. Gravitational lensing by intervening galaxies was postulated as the origin of the effect, but intrinsic absorption could not be ruled out. The gravitational lensing hypothesis was investigated by Holz & Wald (1998), whereas the present work concentrates on the possibility of intrinsic absorption.

As such, the purpose of this work is to attempt a preliminary quantification of the fraction of narrow, but intrinsic C IV absorption in QSOs. If this fraction is anything other than negligible, then studies of absorption line systems will have to be reconsidered. In addition, we comment briefly on the properties of $z_{abs} \approx z_{em}$ absorbers, line-locking, and the effects of gravitational lensing on our analysis. Section 2 briefly describes the data. In §3, we present an analysis of the C IV distribution in velocity space with respect to various QSO properties. In §4 we discuss the implications of our analysis. Section 5 presents our conclusions. In the Appendix, we present a more detailed description of the data.

2. The Data

The data gathered by York et al. (1991) has been updated to include most of the absorption line data in the literature up to 1994 October and some of the more recent data up to 1997. Since the catalog is inhomogeneous, care must be taken to avoid any possible biases in the data. In particular, we correct for known biases by ensuring that all stated results apply for an analysis of only the largest possible “homogeneous” samples, which will be defined later.

Given the possibility of intrinsic absorption and coupling it with the fact that radio-loud and radio-quiet QSOs could be separate populations, one has the potential for some significant biases. Therefore we have undertaken the task of compiling the radio properties of all of the QSOs in the catalog. We have searched the literature for 6 and 20 cm integrated radio flux densities for our objects in order to classify the QSOs as radio-loud (RL) or radio-quiet (RQ) and (for those that are RL) as flat spectrum or steep spectrum. Additionally we have analyzed 20 cm data from the Faint Images of the Radio Sky at Twenty centimeters (FIRST; Becker, White, & Helfand 1995) and NRAO VLA Sky Survey (NVSS; Condon et al. 1998) VLA surveys to determine the 20 cm radio morphology and core-to-lobe ratios of $\sim 1/4$ of the RLQSOs in our database. We then use this information to study the velocity distribution of high-ionization C IV absorption relative to intrinsic QSO properties (redshift, absolute visual magnitude, radio spectral index, and radio morphology).

For a more detailed description of the absorption line data, we refer the reader to York et al. (1991, and references therein). The details regarding the collection and analysis of the intrinsic QSO properties is essential to this work; however, we feel that a discussion of it here would detract from the focus of the paper, and we have chosen to leave that discussion to the Appendix.

3. Analysis and Results

To ensure the reality of the C IV systems used in the analysis of our samples, we have made some stringent cuts on the data. First of all, only systems classified as grade A, B, or C are used. The grading system for the new catalog is derived from that of York et al. (1991), but has been revised to some extent. Herein grades A, B, and C refer to systems with four or more lines, three lines, and two lines, respectively. In addition, we require that both members of the doublet have a rest equivalent width (REW) greater than 0.15\AA to avoid any problems with weak lines appearing preferentially on top of emission lines due to higher signal-to-noise ratio (S/N; Sargent, Boksenberg, & Steidel 1988). Note that this requirement means that grade C (only two lines) systems are “doublet only” systems. This constraint also decreases the probability of the two stronger lines of line-locked systems appearing to be a single system. After all the above cuts have been applied, systems within 250 km s^{-1} of each other are combined (Sargent, Boksenberg, & Steidel 1988). The new redshift is the equivalent width weighted mean of the redshifts of the two systems being merged. If both systems are from the same reference then the rest equivalent widths are summed, and the errors are added in quadrature. If the absorbers are not from the same reference then the REW is given by the error weighted mean of the individual REWs. Finally, all lines are required to be at least 5σ detections.

Then, for each line meeting the above requirements, we determine how many times the absorber could have been seen at this velocity (with this strength) for all of the QSOs in the catalog. This number is then used to normalize the counts, since the bins are not necessarily sampled evenly. See Vanden Berk et al. (1996) for specifics on this normalization process.

The first step of our analysis was to look for systematic differences (between different QSO properties) of the absorber distribution in velocity space (β) relative to the QSOs. For example, if we can assume that the radio spectral indices of the QSOs are unlikely to be affected by the presence of intervening galaxies it would seem reasonable to guess that any systematic trends between radio spectral index and absorber velocity distributions are due to absorption that is intrinsic to the QSO. These systematic differences could be manifested as a change in the normalized number of absorbers per unit velocity difference with respect to the QSO redshift ($dN/d\beta$), as a perturbation in a small velocity range as might be caused by line-locking effects, or as a large scale difference in the shapes of the velocity distribution.

Each QSO was placed into one class of each of the following sets of categories: (1) bright or faint, (2) high redshift or low redshift, (3) radio loud, radio moderate, or radio quiet, (4) flat spectrum or steep spectrum, and (5) core dominated or lobe dominated. The bright/faint division was made by determining the median absolute magnitude of the sample, which is $M_V = -27.0$. High redshift versus low redshift was also found by taking the median of the sample which is $z_{em} = 2.0$. Separation into radio luminosity bins is discussed in the Appendix. For those QSOs with both 6 and 20 cm flux densities we find a median radio spectral index of $\alpha_6^{20} = -0.5$, and we take QSOs with $\alpha < -0.5$ to be steep-spectrum. (N.B. throughout this paper spectral indices (α) are given such that $f_\nu \propto \nu^\alpha$.) Radio morphology was determined by eye on a case by case basis from FIRST contour plots that were kindly provided by R. Becker and also by determining the core-to-lobe ratios using both FIRST and NVSS data from the VLA. See the Appendix for further details regarding the QSO properties.

In addition to comparing all of the absorbers in a single population to all absorbers in another population, we have also done the comparisons after attempting to normalize for other effects. For example we find that the brighter QSOs are statistically at higher redshifts than the fainter QSOs; so how can we be sure that an effect seen in the bright versus faint distribution is not really due to redshift? Obviously we cannot be sure that the redshift is not the cause of the effect unless we have some way of normalizing the

redshift distributions between the bright and faint samples.

In order to handle biases of the type described above, we have devised a naive, yet effective scheme to minimize these effects. Very simply, we force the distribution of a given parameter or parameters to be the same for the two samples we want to compare. This is done by binning the data in the parameter that we want to normalize out and requiring that the same number of each type of QSO appear in each bin. In a given bin, we keep all of the QSOs of the type with the least number in that bin and we randomly select from the complementary QSO population as many QSOs as matches the lesser number. We then make 10 such random catalogs for each pair of properties that we wish to compare. For example, if there are eight bright QSOs in the $2.0 < z_{em} < 2.5$ bin and only five faint QSOs, then our subcatalog will have all five of the faint QSOs and five randomly selected bright QSOs in this redshift bin. We repeat this 10 times, making 10 subcatalogs — each of which are analyzed separately, then the individual results are averaged. The hope is that this will remove any effects of parameters that are not being studied in a given sample. We have every indication that this is working as intended and therefore are comfortable that the reported results are indeed due to the properties in question and not a result of correlations between intrinsic QSO properties.

3.1. Overview of the Large Scale Velocity Distribution of C IV

Previous work (e.g., Young, Sargent, & Boksenberg 1982; Yong & Jian-sheng 1994) has stressed that the distribution of C IV absorbers is uniform in velocity space (at least out to $\beta = 0.238$ where the Lyman α forest makes it difficult to properly identify C IV absorption). This is generally done by showing that the Bahcall-Peebles parameter (Bahcall & Peebles 1969) is distributed smoothly, or by using a Kolmogorov-Smirnov (K-S) test to show that the velocity distribution of absorbers is consistent with a flat distribution. In our analysis we chose to do neither of the above. We feel that the data are too inhomogeneous for either of the Bahcall-Peebles tests (though “Test 2” was designed for inhomogeneous data). As for the K-S test, there is no need to repeat what has already been done numerous times and more importantly we do not believe that doing such a test on our data would yield any new results. That is, we will not argue that the distributions are inconsistent with being flat.

3.2. Bright versus Faint

The distribution of C IV absorption in velocity space with respect to absolute optical magnitude can be seen in Figure 1, where we plot $dN/d\beta [\equiv N(\beta)]$ versus β for intrinsically bright QSOs (*solid line*) and faint QSOs (*dashed line*). Throughout this paper, β is given by

$$\beta = \frac{(1 + z_{em})^2 - (1 + z_{abs})^2}{(1 + z_{em})^2 + (1 + z_{abs})^2}. \quad (1)$$

The total number of absorbers contributing to the normalized histogram is noted for each population and Poisson error bars are given. In these plots All refers to the sample that includes A, B, and C graded absorbers that have been combined within 250 km s^{-1} . In the lower panel the ZR refers to the same sample, but with the redshift (z) and radio luminosity (R) normalized out as per the procedure described in the beginning of §3.

From Figure 1 it is clear there is an excess of absorbers in bright QSOs over faint QSOs from

15,000 km s⁻¹ to 65,000 km s⁻¹ ($0.05 < \beta < 0.2167$) for both samples. The bottom panel shows that if the redshift and radio luminosity distributions are normalized as described above, then the effect still persists, but at smaller significance. In particular, although the higher redshift QSOs in our sample have been shown to be statistically brighter, the bright/faint separation is still evident in the redshift normalized sample.

It is also interesting to note that there is a small peak in the number density of absorbers in bright QSOs near $\beta = 0.1c$. This is near the typical terminal velocity of BAL troughs (Turnshek 1988); however, we have excluded all BALQSOs and possible/probable BALQSOs from our sample. Also the peak is right where one would expect a feature if there were significant line-locking between Si IV and C IV (Burbidge & Burbidge 1975).

Table 1 gives the significance of the differences in two velocity bins for both of the bright/faint samples studied using a simple Student’s t -test (see the Appendix for details). In addition, we determine the significance for 2 other samples. In Table 1 1000 B refers to the sample with A and B graded absorbers that have been combined within 1000 km s⁻¹, whereas 1000 C has A, B, and C graded absorbers. The 1000 C sample is that which most closely resembles the primary sample used by Sargent, Boksenberg, & Steidel (1988). In all, the bright/faint difference is a $\geq 2.74\sigma$ effect, which corresponds to a 99.4% confidence limit (assuming that the error distribution can be considered approximately Gaussian). At velocities $< 15,000$ km s⁻¹ there is no apparent difference in the two populations, and at higher velocities, the faint sample actually shows a small excess.

3.3. Loud versus Quiet

The radio-loud and radio-quiet distributions (Fig. 2) show little difference at zero velocity, whereas there is a small, but significant (3.1σ) excess in RQQSOs out to at least $0.1c$. Again it is interesting that the excess cuts off at about $0.1c$, which is about the terminal velocity of broad absorption troughs, even though we have removed the known BALs from our sample. This excess remains if the redshift (z) and absolute optical magnitude (M) distributions are normalized for the two samples, which means that the excess cannot be the result of a correlation with z_{em} or M_V . From Table 1, we see that combining absorbers within 1000 km s⁻¹ also has little effect on the significance of the excess of absorbers in RQ objects; however, rejection of the “doublet only” (grade C) systems results in no significant difference between the two samples. Nevertheless, there would appear to be a difference in the distributions of absorbers in our primary sample — which poses problems for all the high velocity systems being caused by intervening galaxies.

3.4. High z versus Low z

At first glance, the high redshift and low redshift samples (Fig. 3) also seem to show a difference in their mean values of $dN/d\beta$. However, after normalization of the M_V distribution for the two samples, we find that there is no significant difference between the two samples. Therefore, any apparent excess of absorbers along the line of sight to high redshift QSOs is probably due to the tendency for the high z QSOs to fall into our bright sample. (N.B. the bright/faint differences hold in spite of redshift normalization, so the opposite statement is *not* true.) This lack of change in $dN/d\beta$ for our two different redshift samples is essentially the same as saying that dN/dz is not a function of redshift, since there is no change in the average level of $dN/d\beta$ between our two redshift samples. However, other than the comments made in §4.3, we will not comment further on the relationship between our analysis of $dN/d\beta$ and studies of the evolution

of dN/dz , which is more commonly discussed in the literature. For discussions of the redshift evolution of C IV, see Vanden Berk et al. (1996), Borgeest & Mehlert (1993), or York et al. (1991).

3.5. Steep versus Flat

Perhaps the most striking results of our study come from the comparison of steep-spectrum radio-loud QSOs to flat-spectrum radio-loud QSOs (Figs. 4 and 5). First, there is an apparent excess of C IV absorbers at velocities less than 5000 km s^{-1} ($\beta < 0.0167$) along the line of sight to steep-spectrum sources — an effect that was first reported by Weymann et al. (1979) and confirmed by Foltz et al. (1986). Essentially, Foltz et al. (1986) found that their excess and the lack of an excess in the Young, Sargent, & Boksenberg (1982) analysis for $v < 5000 \text{ km s}^{-1}$ could be explained by the lack of steep-spectrum QSOs in the YSB data set relative to that of Foltz et al. (1986). They also found that these “associated” systems tend to be very strong ($\text{REW} > 1.5 \text{ \AA}$). This excess of associated absorption is quite evident in Figure 6, where we plot REW versus β for C IV absorption systems in both steep- and flat-spectrum QSOs. However, we caution that in Figure 6 the number of absorbers is not normalized by the number of times that they could have been seen.

Upon closer inspection of the top panel of Figure 4 we see that the large scale ($10,000 \text{ km s}^{-1}$ bins) distribution of steep-spectrum absorbers near the QSO is really not significantly greater than that of the flat-spectrum QSOs, but the apparent dearth of higher-velocity absorbers in steep-spectrum QSOs makes the effect appear more significant. In fact, if we normalize the redshift (z), absolute optical magnitude (M) and radio luminosity (R) distributions for the flat and steep QSOs (as in Fig. 4, *bottom*) then we find that there is *no* difference between steep and flat for $\beta < 5000 \text{ km s}^{-1}$. However, on smaller scales (1500 km s^{-1} bins), we do confirm that excess in steep-spectrum sources reported by Foltz et al. (1986). This is an interesting result and deserves further consideration, but it is beyond the scope of this paper and we shall postpone any further discussion.

For absorbers at velocities exceeding 5000 km s^{-1} , both distributions are relatively flat, which is consistent with the intervening galaxy hypothesis; however, there is apparently a significant difference in the mean value of $dN/d\beta$. In particular, there is an excess of absorbers in flat-spectrum objects over absorbers from steep-spectrum objects from 5000 km s^{-1} to at least $25,000 \text{ km s}^{-1}$ if not $55,000 \text{ km s}^{-1}$. For the data that has been cut most stringently, the difference between the average level of $dN/d\beta$ between flat and steep QSOs from 5000 km s^{-1} to $65,000 \text{ km s}^{-1}$ is 2.84 and is a 4.2σ effect. The largest excess is from 5000 km s^{-1} to $25,000 \text{ km s}^{-1}$ for the sample which has been corrected for redshift (z), optical absolute magnitude (M), and radio luminosity (R) effects. Here there are seven more absorbers per unit β , per line of sight in the flat-spectrum QSOs as compared to the steep-spectrum QSOs. As it is difficult to believe that the clouds causing the absorption could significantly affect the radio spectral index, one is left to conclude that these “excess” absorbers are likely to be intrinsic to the QSO.

We have also determined that the QSO spectral indices correlate roughly with radio morphology as is evidenced by comparisons with FIRST 20 cm radio data. This correlation lends credence to the idea that the difference between the flat- and steep-spectrum samples might be due to absorbers in the vicinity of the QSOs. This is important because variability is likely to have a deleterious effect upon our spectral indices, but it is our hope that we have enough data to dampen the effects of variability. It is particularly likely that the flat-spectrum QSOs will be included in the steep-spectrum sample since the orientation of the flat-spectrum QSOs is such that they are more likely to be beamed and thus variable. This hypothesis is

supported by our calculations of core-to-lobe ratios (see the Appendix) where we find that for 35 QSOs with both spectral indices and core-to-lobe ratios, there are 10 core-dominated sources that we have classified as “steep”, but only three lobe-dominated sources that were classified as “flat”. A full analysis is beyond the scope of this paper, but we will revisit the question in the Appendix.

In addition, it is interesting that the majority of the strong C IV systems at large velocities are in flat-spectrum QSOs as can be seen in Figure 6. Since most of the associated systems are strong, Foltz et al. (1986) concluded that the rest equivalent width may be correlated with intrinsic absorption. If this is the case, then the excess of strong systems at high-velocities in flat-spectrum QSOs would certainly be consistent with a population of intrinsic absorbers.

4. Discussion

4.1. Intrinsic Absorption

A number of interesting things regarding intrinsic absorption can be derived from the C IV distributions described above. As noted, the optically bright QSOs do indeed show an excess of absorbers and this is true for $15,000 < v < 65,000 \text{ km s}^{-1}$. This bright excess could be consistent with lensing of the QSOs by intervening galaxies if a suitable lensing scenario could be found. However, there is a similar excess of absorbers in the flat-spectrum QSOs. Flat-spectrum QSOs tend to be brighter than the steep-spectrum QSOs (at least in our sample — see the Appendix), and one might be tempted to conclude that the flat-spectrum excess is merely a residual of the bright excess. We have shown in the bottom panel of Figure 4 that the flat excess still persists even when we normalize the M_V distributions of the flat and steep samples, so it seems unlikely that the flat-spectrum excess is a residual of the bright excess. In any case, it is difficult for gravitational lensing by diffuse intervening galaxies to significantly alter the observed radio spectral index of QSOs and we are inclined to believe that there is a real excess of absorbers in flat-spectrum QSOs that is *not* due to lensing of the type noted. On the other hand, an increase in the optical brightness could reasonably be correlated with a flatter radio spectral index, since the optical light from the core is probably beamed along with the radio flux from the core. Therefore, the bright excess *could* reasonably be a residual of the flat-spectrum excess, which is probably just an orientation effect.

If a significant fraction of the C IV absorbers are indeed intrinsic to the QSO environment, then it would be desirable to explain the above observations with a single model. If we consider just the RLQSOs, and we assume that the spectral index correlates with the orientation of the QSO to our line of sight, we may be able to explain the bright/faint differences as being due to relativistic beaming. Specifically, flat-spectrum QSOs may be expected to be brighter than steep-spectrum QSOs due to beaming of the optical continuum along with the radio continuum (Browne & Wright 1985).

If the clouds causing the absorption are not moving radially with respect to the QSO engine, then orientation (and therefore spectral index) effects might be expected in the velocity distribution of the absorbers. A possible model is one in which the clouds are constrained to move along field lines which are perpendicular to the disk. Figure 7 shows a model (kindly provided by Arie Königl and John Kartje) that depicts the plane of the disk and the magnetic field lines as being perpendicular (see also Fig. 13 in Königl & Kartje 1994). In Figure 7, a line of sight to the central engine that passes through point 2 would generally show a flatter spectrum than a line of sight passing through point 3. However, this is not to say that the locations of points 2 and 3 are indicative of lines of sight that are inherently flat and steep, respectively. If the jet axis is perpendicular to the disk, then we might expect to see fewer high-velocity clouds along the

line of sight to steep-spectrum QSOs as compared to flat-spectrum QSOs, since the velocity vector of the clouds would be seen in projection towards steep-spectrum objects. Specifically, in steep-spectrum QSOs we might expect to see a pileup of C IV near zero velocity if the velocity vectors of the clouds are generally perpendicular to our sight line, or possibly even an evacuated velocity region as a result of clouds moving out of the line of sight.

Another possibility is that the clouds seen in steep-spectrum objects are pushed to higher velocities than clouds in flat-spectrum objects, which might explain the apparent dearth of clouds (in velocity space) towards steep-spectrum QSOs. That is, there might be the same number of clouds towards both types of QSOs, but for some reason the clouds in steep-spectrum objects are more widely distributed in velocity space. Some of these clouds may even be pushed to velocities that would place them in the Lyman α forest, which is beyond the velocity limit of this analysis.

If there were a similar sort of orientation effect for the RQQSOs, then we might be able to explain why the bright/faint difference is stronger than the steep/flat difference. That is, if we had some measure of the orientation of RQQSOs, we might also find a relationship between $d\mathcal{N}/d\beta$ and orientation angle. Then, if for some reason the RQQSOs also showed an optical brightening with increasing angle from the disk, we might expect that the difference between the bright and faint samples in both RL and RQQSOs would be stronger than for the steep versus flat samples in RLQSOs. If this is the case, M_V may serve as a surrogate measure of orientation in the RQ population.

In light of the above discussion, it is interesting to note that the small excess of absorbers in RQQSOs over RLQSOs might also be explained as an orientation effect. If the very flattest of the RL QSOs are classified as BL Lacs (Fig. 7, sight line 1) rather than as QSOs, then this effectively “steepens” the average RL spectral index (or orientation) with respect to the RQ population (assuming that RL and RQQSOs are distinct populations with otherwise similar attributes). Since we also remove BALQSOs from our analysis, there might be a similar biasing of the orientation in RQQSOs. Specifically, if BALQSOs are just normal RQQSOs, but oriented such that the line of sight skims the surface of a surrounding torus that is coplanar with the accretion disk (Fig. 7, sight line 4), then the removal of these QSOs would “flatten” the average spectral index of the RQQSOs in our sample. This would further amplify the difference between our RL and RQ population and the difference between the two might be explained as a difference in the average orientation angle of the two types of QSOs. On the other hand if BALs are observed in an orientation that is more perpendicular to the plane of the disk, then this would not help explain the differences between our RL and RQ samples.

Finally, if we make the naive assumption that all the absorbers at velocities greater than 5000 km s^{-1} in steep-spectrum QSOs are due to intervening galaxies and that the flat-spectrum excess is entirely the result of contamination by intrinsic absorption, then we can make a rough estimate of the fraction of intrinsic C IV absorption. Using the data from our normalized 250 km s^{-1} sample, this method yields 36% as an estimate of the contamination of C IV systems by absorbers that are intrinsic to the QSO. If true, then this certainly has significant consequences for future (and past) studies of QSO absorption line systems. Furthermore, preliminary analysis of our core-to-lobe ratios would seem to indicate a trend between core-to-lobe ratio and C IV absorber velocity distribution. We expect that a full reanalysis using core-to-lobe ratios will reveal that we have mis-classified more flat-spectrum QSOs than steep-spectrum QSOs, which may serve to increase the dichotomy in the absorber velocity distribution between the two populations. If this preliminary observation can be confirmed with a much larger sample, then the fraction of C IV that is intrinsic may be significantly larger.

4.2. Gravitational Lensing

Vanden Berk et al. (1996) showed that there is an excess of C IV absorbers seen along the line of sight to “bright” QSOs and argued that this excess might be the result of each absorber causing a small amount of magnification due to gravitational lensing. However, they could not rule out the possibility that the effect might be caused, at least in part, by intrinsic absorption. Holz & Wald (1998) conducted a study to determine if the effect could indeed be caused by gravitational lensing. They found that even for the most favorable conditions, lensing could only account for a brightening of the QSO by about 0.08 mag per absorber, which is not enough to produce the observed effect, though it is in the right direction. Herein we have considered the alternative possibility, which is that the effect is caused by intrinsic absorption. We find that the existence of a component of C IV absorbers that are intrinsic to the QSO is indeed consistent with the excess of absorbers in bright QSOs as seen by Vanden Berk et al. (1996), and also with the observations presented herein. However, we cannot rule out gravitational lensing (or some other effect) without more data and further analysis.

One caveat is that since gravitational lensing is achromatic, we have naively assumed that lensing by intervening galaxies would affect our 6 and 20 cm flux densities equally, such that lensing could not influence the radio spectral indices of the QSOs. However, it may be possible for lensing to cause a flattening of the spectral index due to the fact that lensing would have a greater effect on light from the core than light from the lobes. For both the core and the lobes considered separately, there will be no relative change in the 6 to 20 cm flux densities due to lensing, but if the core is affected more by lensing then this changes the fraction of the light in the beam that is coming from the core. Since the core generally has a flatter spectrum than the lobes, we might expect to see a flattening of the spectrum as a result of gravitational lensing. Therefore, an excess of absorbers in flat-spectrum QSOs could be indicative of gravitational lensing. This would certainly be in agreement with the fact that our flat-spectrum QSOs are brighter than the steep-spectrum sources by about 0.75 mag. However, it has been found that flat-spectrum sources are generally at least 1 mag brighter than steep-spectrum sources due to relativistic beaming (Browne & Wright 1985). Therefore, unless flat-spectrum QSOs are preferentially lensed, there appears to be no need to invoke gravitational lensing to explain the difference in brightness between our flat-spectrum QSOs and our steep-spectrum QSOs. A detailed comparison of core-to-lobe ratios from 20 cm FIRST maps between our sample of QSOs and all the QSOs found in the FIRST survey may allow us to make a more definite conclusion.

4.3. dN/dz versus $dN/d\beta$

Since it has become common to assume that absorption systems with $v > 5000 \text{ km s}^{-1}$ are due to intervening galaxies, it has also become common to use dN/dz to study the evolution of absorbers in redshift. Whatever one’s opinions are in terms of whether it is more appropriate to study absorption systems in redshift space or velocity space, it is worth taking a moment to consider the differences in the two selection functions (i.e. the number of times an absorber *could* have been seen at a given redshift or velocity). For the majority of the QSOs in our catalog, the C IV emission line is seen. In terms of the C IV absorbers, this means that the selection function has a maximum near zero velocity and decreases smoothly with increasing velocity. This means that the $dN/d\beta$ selection function is relatively flat (at least out to the velocity of the Lyman α emission line, $v \approx 0.238c$). Thus, the process of normalizing the number of absorbers observed by the number of times an absorber could have been seen at that velocity is unlikely to produce strong, artificial features.

On the other hand, the selection function for $d\mathcal{N}/dz$ is generally *not* flat, since for any given data set there is usually a peak in the redshift distribution. In our data set, the selection function is not very smooth as a result of the combination of many surveys into one. The result is that small errors in either the observed distribution of absorbers with respect to redshift and/or the number of times an absorber could have been detected at a given redshift, can produce large deviations from the true value of $d\mathcal{N}/dz$. This is particularly true at the edges of the selection function. Although this is by no means an argument for the intrinsic nature of C IV absorbers, we do feel that it is important to point out that an analysis of the distribution of absorbers in redshift space is much more complicated than the same analysis in velocity space.

4.4. Associated Absorption

We explained that there is apparently no significant difference in $d\mathcal{N}/d\beta$ (using a single $10,000 \text{ km s}^{-1}$ bin) for $v < 5000 \text{ km s}^{-1}$ for any two QSO properties after having properly removed the effects of other QSO properties. Although this is seemingly in contrast with other work, we emphasize that the velocity scale studied here is quite different from that studied by Foltz et al. (1986), whose work we verify if we use 1500 km s^{-1} bins. In addition, the similarity between the steep and flat $d\mathcal{N}/d\beta$ levels could be an artifact of the fact that our steep/flat dividing line is unphysically motivated. If so, there might be a real difference in the associated population between steep- and flat-spectrum QSOs, but it is masked because we allow steep-spectrum QSOs to creep into our flat-spectrum sample. We hope to revisit this problem using radio core-to-lobe ratios as a measure of orientation in place of radio spectral indices.

However, if there really is no large scale difference in the overall level of $d\mathcal{N}/d\beta$ for absorbers with velocities less than 5000 km s^{-1} , then this symmetry is consistent with the associated absorber population being composed of virialized material (such as might be caused by a cluster surrounding the QSO), since the orientation of the QSO should not have any significant impact on the distribution of a virialized population. Again, this should be considered in more detail, but it is beyond the scope of this paper.

4.5. Line-locking

This study was initially motivated in part as a search for line-locking in our absorption line catalog. Despite that fact that we have much more data than was considered in the Burbidge & Burbidge (1975) study, we still find it difficult to do a proper study of line-locking. We estimate that 5 times as many data are necessary to properly study emission-absorption line-locking and 60 times as many data are required for a detailed study of absorption-absorption line-locking. The data from the Sloan Digital Sky Survey should certainly provide the quantity and quality of data needed for such studies. However, even in the current data set there are certainly hints of line-locking features (e.g., peaks near $0.1c$) and we hope to pursue a full analysis at a later date. For now, we have chosen to concern ourselves with the large scale velocity distribution of the absorbers for which we have much better statistics.

5. Conclusion

We have analyzed the velocity distribution of C IV absorption line systems in terms of intrinsic QSO properties for the largest compiled sample of C IV systems. This data set is a compendium of the data in the literature and as such is indisputably heterogeneous; however, great care has been taken to ensure that our results are not dependent upon any known biases in our catalog.

Our conclusions regarding the distribution of C IV absorbers at velocities exceeding 5000 km s^{-1} can be summarized as follows:

1. There appears to be no significant change of the C IV velocity distribution with respect to redshift, which is consistent with dN/dz being independent of redshift.
2. Optically bright QSOs show an excess of C IV absorption from $15,000 \text{ km s}^{-1}$ to $65,000 \text{ km s}^{-1}$ (relative to the emission-lines), with a peak near $\beta = 0.1c$.
3. We find an excess of absorption systems in radio-quiet QSOs over radio-loud QSOs out to velocities of $30,000 \text{ km s}^{-1}$, which is curiously near the average terminal velocity of broad absorption lines in BALQSOs — despite the fact that we have excluded BALQSOs from our analysis.
4. There is an excess of C IV absorption line systems in flat-spectrum, radio-loud QSOs, with an accompanying dearth in steep-spectrum radio-loud QSOs. This excess is strongest from 5000 km s^{-1} to $25,000 \text{ km s}^{-1}$, but may extend all the way to the Lyman α forest at $\beta = 0.238$. Preliminary analysis of 20 cm data from the FIRST VLA Survey corroborates the assumption that spectral index is roughly correlated with QSO orientation.
5. If the observed difference in the flat-spectrum distribution as compared to the steep-spectrum distribution is due to orientation-dependent intrinsic absorption then we conclude that a significant fraction ($\sim 36\%$) of C IV may actually be intrinsic to the QSOs and not due to intervening galaxies.
6. The use of core-to-lobe ratios instead of spectral indices is likely to allow for a better determination of the fraction of intrinsic C IV absorption. The few data we have now support the observed differences in steep versus flat-spectrum QSOs and may indicate an even larger fraction of intrinsic absorption.

Although it is possible that part of these observed effects might be the result of gravitational lensing of QSOs by galaxies producing absorption line signatures, we find that the observed results can be explained without having to invoke the lensing hypothesis. If the velocity distribution of these clouds is not spherically symmetric, then the observed results may not be unreasonable. In particular, the excess of absorbers in flat-spectrum, optically bright and radio-quiet QSOs may be a results of relativistic beaming and orientation effects.

Regardless of what causes the observed differences in the C IV distributions, it is noteworthy that there are any differences at all. Serious consideration must be given to the consequences for studies of QSOALS if these results can be confirmed with more homogeneous data sets. In particular, we stress the need for QSO absorption line surveys with more uniform distributions of radio properties and fainter magnitude limits. Such surveys would help discriminate between real effects of intrinsic absorbers as opposed to effects resulting from using magnitude-limited samples with biased radio properties.

A large number of people deserve our thanks for contributions they have made to this work, including: Bob Becker for providing FIRST 20 cm contour plots and for discussions regarding the radio analysis, Gary

Sowinski for help classifying the BAL properties of our QSOs, Jean Quashnock for discussions regarding statistical analysis, Arie H. Königl and John Kartje for discussions regarding terminal velocities of BAL clouds and BAL models, Chris Mallouris and Damian Bruni for their efforts in updating the catalog, Arlin Crotts for discussions regarding the binning of data with different velocity resolution, and an anonymous referee for suggestions that helped clarify the paper. This research has made use of the NASA/IPAC Extragalactic Database (NED) which is operated by the Jet Propulsion Laboratory, California Institute of Technology, under contract with the National Aeronautics and Space Administration.

A. Cataloging Radio Data

The radio data in the catalog has been compiled as follows. First we searched for matches between QSOs in our absorption line catalog and the catalog of strong 1.4 GHz sources produced by White & Becker (1992) from the Green Bank 1.4 GHz Northern Sky Survey (Condon & Broderick 1985; Condon & Broderick 1986). Any QSO within $160''$ of a radio source was taken as a match; matches with separations much larger than $30''$ were confirmed with NED⁴. This radio catalog has the useful property that the authors have cross-correlated it with their 4.85 GHz catalog (Becker, White, & Edwards 1991) made from the Green Bank 4.85 GHz Northern Sky Survey (Condon, Broderick, & Seielstad 1989), so that many of the sources have not only 20 cm flux densities, but also 6 cm flux densities and therefore a 6 to 20 cm radio spectral index. White & Becker (1992) estimate that a comparison of sources in the 1.4 GHz catalog with those in the 4.85 GHz catalog for sources separated by less than $300''$ will result in $\approx 1.4\%$ of such matches being chance coincidences. It is expected that the matches between our optical positions and their radio positions using a radius of $160''$ (the 90% confidence limit on the radio positions) will result in very few spurious matches.

We then updated the 6 cm fluxes found above with those from the GB6 Catalog (Gregory et al. 1996); nondetections within the area covered by the GB6 catalog were assigned upper limits from this catalog. The 20 cm data was then supplemented from both the NVSS (Condon et al. 1998) and FIRST (Becker, White, & Helfand 1995) 20 cm VLA surveys. Specifically, we used the integrated flux densities from the NVSS survey (which covers the whole sky north of -40 degrees in declination) as this quantity should be close to the peak flux density as measured at Green Bank. Comparison of the two data sets bears out this hypothesis. Nondetections within the NVSS boundary were assigned upper limits of 2.5 mJy. We then searched the FIRST catalog to improve our flux density limits wherever possible, since it has a smaller flux density limit. However, detections from the FIRST catalog have not been used, since the Green Bank data is at much lower resolution than the FIRST data.

B. RL versus RQ Determination

Historically the division between radio-quiet and radio-loud QSOs has been determined by either the ratio of the radio flux at 6 cm to the optical flux at 2500 \AA , or by the 6 cm radio luminosity alone. In attempting to classify the QSOs in the catalog we have encountered a number of problems with using these methods and/or wavelengths. As a result we define a slightly different set of criteria which are discussed

⁴The NASA/IPAC Extragalactic Database (NED) is operated by the Jet Propulsion Laboratory, California Institute of Technology, under contract with the National Aeronautics and Space Administration.

herein.

Taking the mean QSO redshift, $\bar{z}_{em} \simeq 2.0$, and the mean B magnitude, $\bar{B} \simeq 18.1$, (taking $B-V = 0.3$) of our catalog, along with a radio spectral index of $\alpha_{rad} \simeq -0.5$ and an optical spectral index of $\alpha_{opt} \simeq -1.0$, then using the traditional formula for the ratio of radio and optical flux densities:

$$\log R^* = \log f(5 \text{ GHz}) - \log f(2500 \text{ \AA}), \quad (\text{B1})$$

where

$$\log f(5 \text{ GHz}) = -29.0 + \log S_\nu + \alpha_{rad} \log(5/\nu) - (1 + \alpha_{rad}) \log(1 + z_{em}), \quad (\text{B2})$$

and

$$\log f(2500 \text{ \AA}) = -22.62 - 0.4B, \quad (\text{B3})$$

(Stocke et al. 1992) then we find that a 6 cm flux density as low as 2.43 mJy will give a value of $\log R^*$ equal to 1.0 — the value often taken as the dividing line between RL and RQ.

This would not be a problem except that the largest, most uniform 6 cm catalog to date, the GB6 catalog from Green Bank (Gregory et al. 1996), has a flux limit of 18 mJy *at best*. Thus, using this catalog alone would result in few (if any) RQQSOs. However, this is not the case at 20 cm. Between the FIRST and NVSS VLA surveys at 20 cm, most of the sky has been covered to flux density limits of at least 2.5 mJy. Therefore we chose to use 20 cm luminosity as our measure of radio strength rather than 6 cm luminosity with the realization that the two wavelengths are likely to sample somewhat different properties. Also, we chose to use the radio luminosity rather than a ratio of radio to optical flux to avoid potential biases caused by partial absorption of the optical flux without an accompanying loss of radio flux.

The equation for computing the radio flux density at 20 cm in mJy (in the rest frame) is

$$\log f(1.4 \text{ GHz}) = \log S_\nu + \alpha_{rad} \log(1.4/\nu) - (1 + \alpha_{rad}) \log(1 + z_{em}). \quad (\text{B4})$$

Where possible we use the measured flux density at 20 cm and the measured 6 to 20 cm spectral index. However, if the 20 cm flux density was not available but the 6 cm flux density was, then we used the 6 cm value with the median radio spectral index ($\alpha_{rad} \simeq -0.5$).

The uncertainty in $\log f(1.4 \text{ GHz})$ due to errors in the spectral index and errors in the radio measurements is

$$\sigma_{\log f(1.4 \text{ GHz})} = \sqrt{\frac{\sigma_{S_\nu}^2}{S_\nu^2} + \sigma_{\alpha_{rad}}^2 (\log(1.4/4.85))^2 + \sigma_{\alpha_{rad}}^2 (\log(1 + z))^2}. \quad (\text{B5})$$

At the median redshift of the catalog, $z_{em} \simeq 2.0$ and assuming 20% error in the radio measurements, and an error in α_{rad} of $\sigma_{\alpha_{rad}} \approx 0.5$, the error is $\sigma_{\log f(1.4 \text{ GHz})} \simeq 0.4$.

The intrinsic, monochromatic luminosity L is then given by

$$\log L \text{ (ergs/s/Hz)} = \log f \text{ (mJy)} - 26.0 + \log(4\pi) + 2 \log D \text{ (cm)}. \quad (\text{B6})$$

For the computation of luminosity distances from redshifts, we have taken $H_o = 65 \text{ km/s/Mpc}$ and $q_o = 0.5$, so that

$$D = \frac{2c}{H_o} \left[1 + z - (1 + z)^{1/2} \right]. \quad (\text{B7})$$

The error in the last term of the luminosity equation is then given by

$$\left[\left(\frac{2}{D} \right)^2 \left(\sigma_{H_o}^2 \frac{D^2}{H_o^2} + \sigma_z^2 \left[\frac{2c}{H_o} \left(1 - 0.5 (1+z)^{-1/2} \right) \right]^2 \right) \right]^{1/2}, \quad (\text{B8})$$

which comes out to about 0.20 with the assumption of a 10% error in the Hubble constant, $\sigma_z = 0.001$, and $z_{em} = 2$.

We use these errors to minimize confusion of RQ and RL sources at the weak detection limit. If one were to take a specific value of $\log L_{rad}$ and say that QSOs above some value are loud and those below that same value are quiet, then given the magnitude of the error calculated above, one can see that a good number of QSOs may be misclassified. However, one can choose instead to have *two* dividing lines such that QSOs below a certain value are quiet and QSOs above another value are loud, whereas QSOs lying between are either moderate in radio strength or are displaced from their proper classification by errors. If we set these two lines such that they are separated by at least 2σ , then we can say (to 95% confidence) that we have not classified anything as RL that is really RQ and vice versa.

An examination of the distribution of radio luminosities with respect to absolute optical magnitude (Fig. 8) has led us to conclude that the easiest way to split our sample of QSOs into RQ and RL populations is to use a straight cut in radio luminosity. By visual inspection of a histogram of the data, we find that the minimum between the two distributions is about $\log L_{rad} (\text{ergs/s/Hz}) = 33.25$ (at 20 cm), which is comparable to the 6 cm value of $\log L_{rad} (\text{W/Hz}) \simeq 26$ (modulo the choice of units), which has been used by previous authors (e.g., Stocke et al. 1992). We have shown above that the error in the log of the radio flux density is on the order of 0.4. If we assume that variability and conversion to luminosity account for an additional error of order 0.2, then we find that the total error in the log of the radio luminosity, $\sigma_{\log L_{rad}}$, is about 0.45. Thus radio-quiet QSOs in our sample have detections or upper limits below 32.80 ergs/s/Hz, whereas radio-loud QSOs are those with detections above 33.70 ergs/s/Hz, such that the two populations are separated by 2σ (Fig. 8). Therefore we can state to 95% confidence that no quiet object has been classified as loud and vice versa. QSOs falling between the two dividing lines are classified as radio-moderate and will be treated separately in our analysis of absorption properties. Upper limits falling in the radio-loud regime (there are only four such points) will also be treated separately, since it is quite possible that better radio data will show that these are actually radio-quiet.

There is at least one potential problem with this division between loud and quiet. The dividing line between moderate and quiet is such that there are few very high redshift radio-quiet QSOs, which is a potential source of bias. In fact, 27 of the upper limits at $z > 3.5$ are just above our RQ cutoff line. However, there are very few (five) radio-loud QSOs with similar redshifts. Essentially, this has the effect of reducing the maximum redshift that we can probe during the course of this study to $z_{em} \approx 3.2$.

C. Other QSO Properties

In addition to radio luminosity, we compare the C IV absorption line distributions to the QSO emission redshift, absolute optical magnitude, 6 to 20 cm radio spectral index, and 20 cm radio morphology.

The absolute optical magnitudes are determined using an optical spectral index $\alpha_{opt} \simeq -1.0$ and

$$M_V = V + 5.0 - 5.0 \log(D) + 2.5(1 + \alpha_{opt}) \log(1 + z_{em}), \quad (\text{C1})$$

where the V magnitude and emission redshift are taken from the literature. Again, the distances have been calculated using $H_o = 65 \text{ km/s/Mpc}$ and $q_o = 0.5$. Note that the apparent magnitude used is not always V, but may sometimes be B or R. Unfortunately, sources of apparent magnitudes don't always clearly indicate to which filter the reported magnitude refers. In these cases we assume a flat optical spectrum and take $V=B=R$ (though we still use $\alpha_{opt} \simeq -1.0$ for the K-correction term). The errors incurred by this process are small ($< 0.1 \text{ mag}$) and are generally less than errors due to measurement and variability and should not affect our results. In addition, the use of filters other than V is normally done in a way that is appropriate to our assumption of $B=V=R$. For example, the R filter is often used to observe high redshift QSOs, where the V band would sample the Lyman α forest, but the R band samples rest wavelengths similar to that of the V band at lower redshifts. The median absolute magnitude for our sample is $M_V \simeq -27.0$.

Radio spectral indices are calculated for all QSOs having detections at both 6 and 20 cm, where

$$\alpha_6^{20} = -\frac{\log(f_6(\text{mJy})) - \log(f_{20}(\text{mJy}))}{\log(\nu_{20}) - \log(\nu_6)}. \quad (\text{C2})$$

The median spectral index for the 262 sources with both 6 and 20 cm measurements is $\alpha_6^{20} \simeq -0.5 \pm 0.5$, where the error is the one sigma deviation for all the data (though it is not a Gaussian distribution).

Of the 262 QSOs with measured radio spectral indices, about one-quarter are within the area of the FIRST Survey. R. Becker has kindly provided us with these maps and we have classified each object by eye as core dominated or not core dominated without any a priori knowledge of the other QSO properties. We find that 17 are core dominated, whereas 21 are not, with the remaining being uncertain. For the core dominated sources the mean spectral index is -0.33 ± 0.45 and the noncore sources have -0.74 ± 0.37 . Although the difference between the two populations is indistinguishable within the errors, it is comforting to find that core-dominated sources generally have a spectrum that is flatter than non-core sources as would be expected from orientation effects in unified models (Antonucci 1993). We have taken $\alpha_6^{20} = -0.5$ as the dividing line between steep and flat — a choice which is apparently born out by the mean core and non core values quoted above, but is otherwise nonphysical.

In an effort to cross check our results obtained using radio spectral indices as a measure of orientation and our preliminary classification of FIRST sources as either core or lobe dominated, we have also calculated radio core-to-lobe ratios for our sample of QSOs. We use the FIRST 5'' resolution survey for our core radio flux density values and the lower resolution (45'') NVSS data to estimate the total flux density from each source. The lobe flux density is then taken to be the difference between the NVSS total and FIRST core flux densities. Our values of R may be affected by variability between the epochs of the FIRST and NVSS observations, but this effect should be relatively small and produce no spurious trends in the data as a source is equally likely to be in a high state either during the FIRST or NVSS observations and hence produce slightly high or low values of R equally as often.

The radio core-to-lobe ratio, $R=S_{\text{core}}/S_{\text{lobe}}$, is a good indicator of relative orientation of similar classes of active galactic nuclei (AGNs; e.g., Orr and Browne 1982). Although lobe flux originates many kiloparsecs from the central engine, core flux is dominated by emission from the inner jet and is likely beamed. Lobe emission is largely independent of source orientation, but the strength of core flux is sensitive to the angle that the jet axis makes with the line-of-sight becoming greatly enhanced at small orientation angles. All other parameters being equal, the observed core-to-lobe ratio should therefore be largest for those objects with jets oriented at the smallest line-of-sight angles.

We computed R only for spatially resolved sources. Sources which are spatially unresolved are, almost certainly, highly core dominated sources, although it is difficult to determine actual upper limits to the core

dominance parameter. Of the 124 quasars considered, 59 were detected by both radio surveys and 35 of these are resolved. All sources were examined visually in order to assure that multiple radio components were properly identified.

These core-to-lobe ratio calculations generally confirm the expected trend between core-to-lobe ratios and spectral indices, though there are a number of exceptions that are likely to be due to variability. Of those that we classified as steep spectrum, 16 are lobe dominated as expected, but 10 are core dominated. For those QSOs that we consider to be flat-spectrum, six are core dominated as expected, whereas three are lobe dominated. Therefore 13 of the 35 QSOs may be misclassified in terms of their spectral indices, whereas the remaining 22 core-to-lobe ratios are in good agreement with the spectral indices. A full reanalysis of the QSO orientation using core-to-lobe ratios is beyond the scope of this paper and will be reserved for future work.

Although we have not intended to include Broad Absorption Line QSOs (BALQSOs) in the catalog, the large amount of attention that the BAL phenomenon has been given in recent years (e.g., Weymann 1995, and references therein) almost ensures that some of our QSOs will acquire the BAL label. Previous studies using data from the catalog have not purposely included the known BALs; however, we have found that recent lists of BAL or suspected BAL QSOs have slightly more objects in common with our catalog than was previously thought. As a result, we have taken the time to classify all the QSOs in the catalog as BAL, probable/possible BAL, CAAL (QSOs with Complex Associated Absorption Lines), probable/possible CAAL, and not any of the above using a version of the BALQSO catalog produced by Sowinski, Schmidt, & Hines (1997).

D. Discussion of QSO Properties

From Figure 8 it is obvious that there is a dichotomy between RLQSOs and RQQSOs as has been reported numerous times in the literature (e.g., Kellermann et al. 1989). It is reassuring that we are able to repeat the separation of the populations and that our dividing line between the two species is close to that used by other authors, even though we use slightly different methods. One striking fact is that there are about as many radio-loud QSOs in our sample as radio-quiet QSOs, despite the fact that radio-loud QSOs are only supposed to be about 10% of the QSO population (Sramek & Weedman 1980). Although it is certainly possible that some of this is the result of mismatches between the optical and radio identifications from our literature search for radio measurements, it is exceedingly unlikely that this would cause the fraction of RLQSOs to go from 10% to over 50%. However, the fraction of radio-loud QSOs is seen to increase considerably for the brightest sources (Hooper et al. 1995). Thus we would expect a fraction larger than 10% in a population of QSOs selected as targets for spectroscopy, since these are likely to be the brightest QSOs. Even so, it is not quite clear why the fraction should be near 50%. One possible explanation may be that those studying QSO absorption lines have the tendency to try to observe equal numbers of each type of QSO (at least in the aggregate of all observers) and this is the cause of the excess of RLQSOs in our sample. Whatever the cause, it seems worth noting this discrepancy.

In Figure 9 we show the distribution of M_V versus the emission redshift of the QSO. The RQ population tends to be brighter than the RL population. In addition, there is a lack of faint objects at high redshifts which is to be expected as a result of flux limited surveys of QSOs. There is also an absence of bright objects at low redshifts, which is probably due to the small volume sampled at lower redshifts and/or some sort of luminosity or density evolution.

We have applied the Student’s t -test (Press et al. 1995) to see if the observed differences are indeed significant. Student’s t is essentially the number of standard errors that the difference in two means deviates from the null hypothesis (that there is no difference in the mean) and the probability is that of randomly obtaining a value of Student’s t that is at least as large as t . We have first made cuts at $z = 3$ and $M_V = -26.0$ to correct for the apparent dearth of faint, high redshift objects that is caused by the limiting magnitude of the data. The redshift difference for the bright versus faint samples is $\Delta z = 0.342$ with a Student’s t of 4.83 and a probability of 6.2×10^{-6} . Similarly, the absolute magnitude difference between the high and low redshift samples is -0.39 mag with a Student’s t of 4.6 and probability 1.5×10^{-5} .

There are also significant differences in the radio-loud (indicated by squares in Fig. 9) and the radio-quiet (indicated by arrows) populations. The average redshift of the RL sample is 1.76, whereas for the RQ sample it is 2.28. The difference has a Student’s t value of 7.14 with probability 7.6×10^{-11} . Also, the RL sample has an average M_V of -26.68 , whereas the RQ value is -27.21 ; this difference has a probability of 1.49×10^{-6} for a Student’s t of 5.07. On the other hand, for RLQSOs we find that there is no significant difference in the radio luminosities of the optically bright versus faint samples, in agreement with Hooper et al. (1995). However, we do find a small difference in the radio luminosities of the high z versus low z samples with a Student’s t of 3.02 and a probability of 3.7×10^{-3} .

The distribution of radio spectral indices is plotted against absolute optical magnitude in Figure 10. There appears to be an excess of faint sources that are steep-spectrum and an accompanying dearth of bright, steep-spectrum sources. This is unusual since although it may be harder to find lobe dominated steep-spectrum objects at high redshifts, there should be no such bias against finding bright steep-spectrum objects; however, it is possible that this effect is intrinsic to the QSOs and is not an observational bias. On the other hand, flat-spectrum QSOs seem to be fairly evenly distributed between bright and faint.

Statistically we find that the steep-spectrum QSOs are fainter than the flat-spectrum QSOs by 0.73 mag, which gives a Student’s t of 5.57 and a probability of 4.8×10^{-7} . The difference in spectral index between the bright and faint samples is 0.25 with a Student’s t of 4.32 and probability 5.8×10^{-5} . The linear correlation coefficient between the spectral index and absolute magnitude is -0.33 .

Finally we plot radio spectral index versus redshift in Figure 11. Here, we find that each quadrant is populated with similar numbers of objects except for very high redshift, steep-spectrum objects which we expect to be underpopulated in flux limited samples due to surface brightness effects. However, if we consider the distribution of spectral index versus redshift and we take only QSOs with $z < 3$ to correct for this lack of lobe-dominated, high redshift QSOs, we find no significant difference in the redshift of the steep versus flat samples, nor in the spectral index of the high redshift versus low redshift samples.

REFERENCES

- Anderson, S. F., Weymann, R. J., Foltz, C. B., & Chaffee, Jr., F. H. 1987, *AJ*, 94, 278
- Antonucci, R. 1993, *ARA&A*, 31, 473
- Arav, N., Li, Z., & Begelman, M. C. 1994, *ApJ*, 432, 62
- Bahcall, J. N., & Peebles, P. J. E. 1969, *ApJ*, 156, L7
- Bahcall, J. N., & Salpeter, E. E. 1966, *ApJ*, 144, 847
- Barlow, T. A., Hamann, F., & Sargent, W. L. W. 1997, in *ASP Conf. Ser. 128, Mass Ejection from Active Galactic Nuclei*, ed. R.J. Weymann, N. Arav, & I. Shlosman (San Francisco: ASP), 13
- Becker, R. H., White, R. L., & Edwards, A. L. 1991, *ApJS*, 75, 1
- Becker, R. H., White, R. L., & Helfand, D. J. 1995, *ApJ*, 450, 559
- Borgeest, U., & Mehlert, D. J. 1993, *A&A*, 275, L21
- Browne, I. W. A., & Wright, A. E. 1985, *MNRAS*, 213, 97
- Burbidge, E. M., & Burbidge, G. R. 1975, *ApJ*, 202, 287
- Burbidge, E. M., Lynds, C. R., & Burbidge, G. R. 1966, *ApJ*, 144, 447
- Condon, J. J., & Broderick, J. J. 1985, *AJ*, 90, 2540
- Condon, J. J., & Broderick, J. J. 1986, *AJ*, 91, 1051
- Condon, J. J., Broderick, J. J., & Seielstad, G. A. 1989, *AJ*, 97, 1064
- Condon, J. J., Cotton, W. D., Greisen, E. W., Yin, Q. F., Perley, R. A., Taylor, G. B., & Broderick, J. J. 1998, *AJ*, 115, 1693
- Foltz, C. B., Chaffee, Jr., F. H., Weymann, R. J., & Anderson, S. F. 1988, in *QSO Absorption Lines: Probing the Universe*, ed. C. Blades, C. Norman, & D. Turnshek (Cambridge: Cambridge University Press), 53
- Foltz, C. B., Weymann, R. J., Peterson, B. M., Sun, L., Malkan, M. A., & Chaffee, Jr., F. H. 1986, *ApJ*, 307, 504
- Gregory, P. C., Scott, W. K., Douglas, K., & Condon, J. J. 1996, *ApJS*, 103, 427
- Hamann, F., Barlow, T. A., Cohen, R. D., Junkkarinen, V., & Burbidge, E. M. 1997, in *ASP Conf. Ser. 128, Mass Ejection from Active Galactic Nuclei*, ed. R.J. Weymann, N. Arav, & I. Shlosman (San Francisco: ASP), 19
- Holz, D. E., & Wald, R. 1998, *Phys. Rev. D*, 063501
- Hooper, E. J., Impey, C. D., Foltz, C. B., & Hewett, P. C. 1995, *ApJ*, 445, 62
- Jannuzi, B. T., et al. 1996, *ApJ*, 470, L11
- Kellermann, K. I., Sramek, R., Schmidt, M., Shaffer, D. B., & Green, R. 1989, *AJ*, 98, 1195

- Königl, A., & Kartje, J. F. 1994, *ApJ*, 434, 446
- Orr, M. J., & Browne, I. W. A. 1982, *MNRAS*, 200, 1067
- Perry, J. J., Burbidge, E. M., & Burbidge, G. R. 1978, *PASP*, 90, 337
- Petitjean, P., Rauch, M., & Carswell, R. F. 1994, *A&A*, 291, 29
- Press, W. H., Teukolsky, S. A., Vetterling, W. T., & Flannery, B. P. 1995, *Numerical Recipes in C* (Cambridge: Cambridge University Press)
- Sargent, W. L. W., Boksenberg, A., & Steidel, C. C. 1988, *ApJS*, 68, 539
- Sowinski, L. G., Schmidt, G. D., & Hines, D. C. 1997, in *ASP Conf. Ser. 128, Mass Ejection from Active Galactic Nuclei*, ed. R.J. Weymann, N. Arav, & I. Shlosman (San Francisco: ASP), 305
- Sramek, R. A., & Weedman, D. W. 1980, *ApJ*, 238, 435
- Steidel, C. C. 1990, *ApJS*, 72, 1
- Stocke, J. T., Morris, S. L., Weymann, R. J., & Foltz, C. B. 1992, *ApJ*, 396, 487
- Stockton, A. N., & Lynds, C. R. 1966, *ApJ*, 144, 451
- Turnshek, D. A. 1988, in *QSO Absorption Lines: Probing the Universe*, ed. C. Blades, C. Norman, & D. Turnshek (Cambridge: Cambridge University Press), 17
- Vanden Berk, D. E., Quashnock, J. M., York, D. G., & Yanny, B. 1996, *ApJ*, 469, 78
- Weymann, R. 1995, in *QSO Absorption Lines: Proceedings of the ESO Workshop*, ed. G. Meylan (Garching, Germany: Springer-Verlag), 214
- Weymann, R. J., Williams, R. E., Peterson, B. M., & Turnshek, D. A. 1979, *ApJ*, 234, 33
- White, R. L., & Becker, R. H. 1992, *ApJS*, 79, 331
- Yong, L., & Jian-sheng, C. 1994, *Chinese Astronomy*, 18, 29
- York, D., Yanny, B., Crotts, A., Carilli, C., Garrison, E., & Matheson, L. 1991, *MNRAS*, 250, 24
- Young, P., Sargent, W. L. W., & Boksenberg, A. 1982, *ApJS*, 48, 455

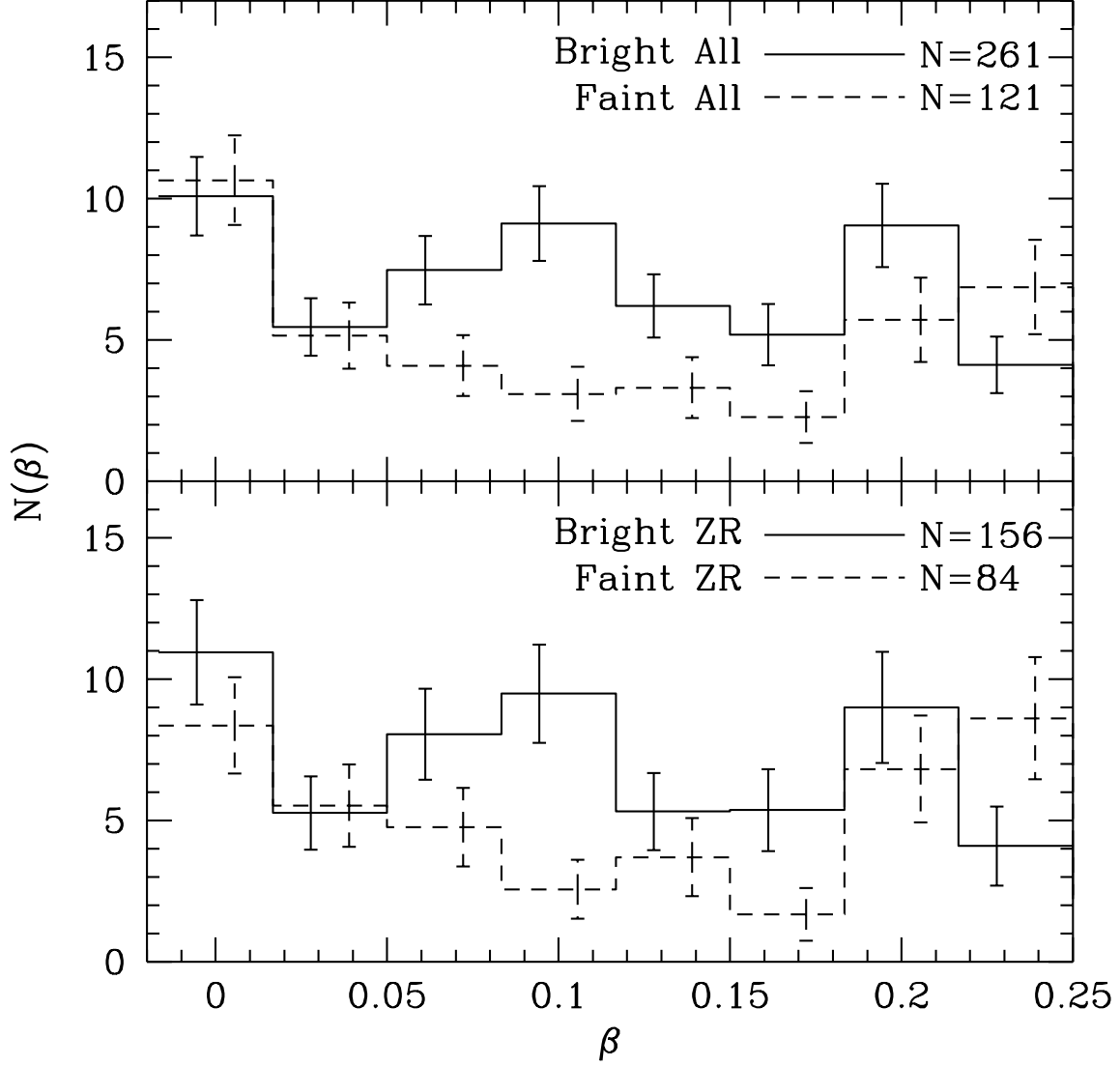


Fig. 1.— Normalized velocity distribution of C IV absorbers for bright and faint QSOs. *Top*: All absorbers graded A,B, or C and combined within 250 km s^{-1} . *Bottom*: Same sample but with the redshift (z) and radio luminosity (R) distributions forced to be the same for both the bright and faint samples. The bright sample is given by the solid line, whereas the dashed line is for the faint sample. The number of absorbers in each sample is indicated in the upper right-hand corner.

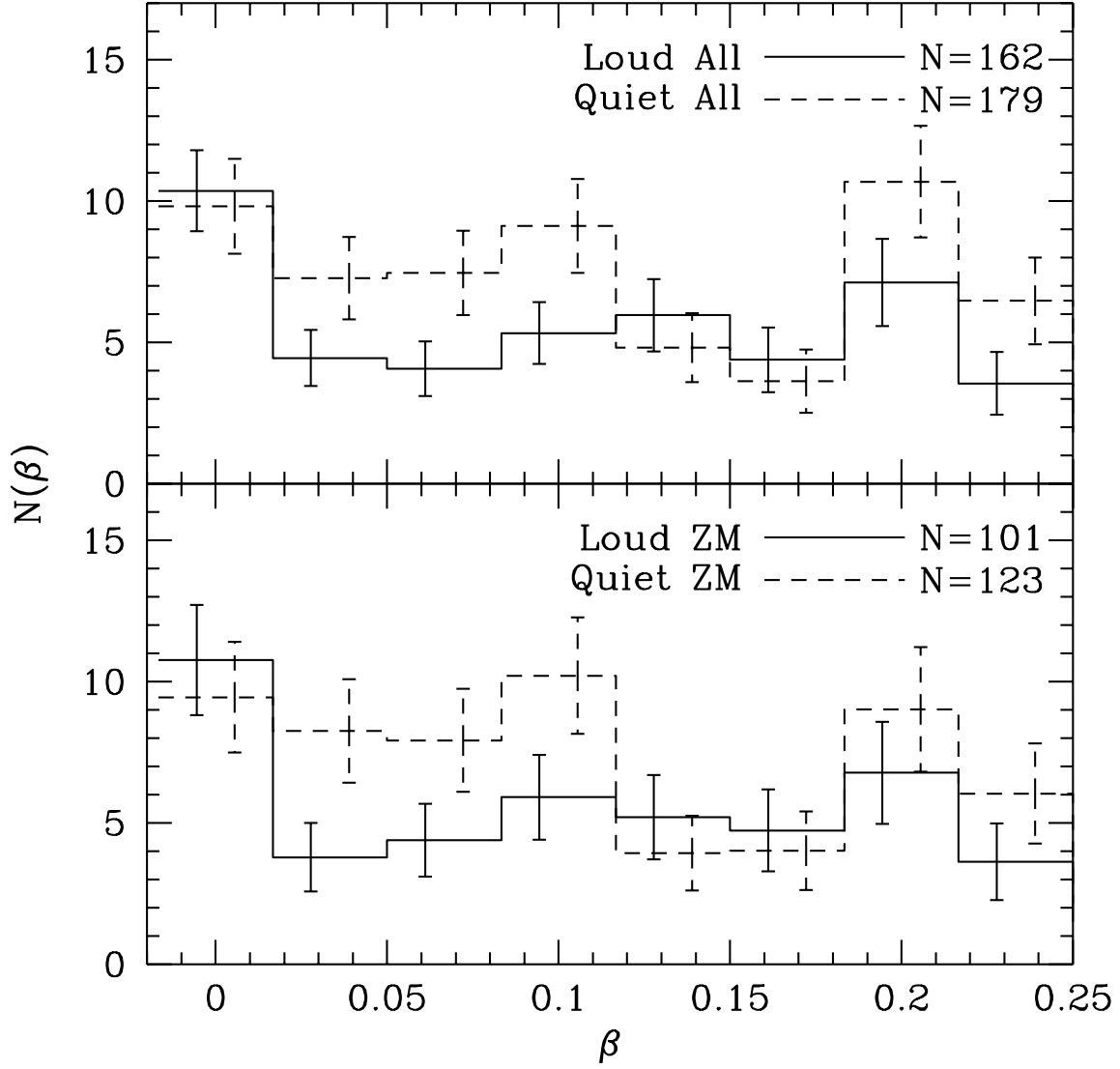


Fig. 2.— Same as for Fig. 1 but for radio-loud and radio-quiet QSOs. ZM in the lower panel refers to the fact that z_{em} and M_V are normalized for this sample.

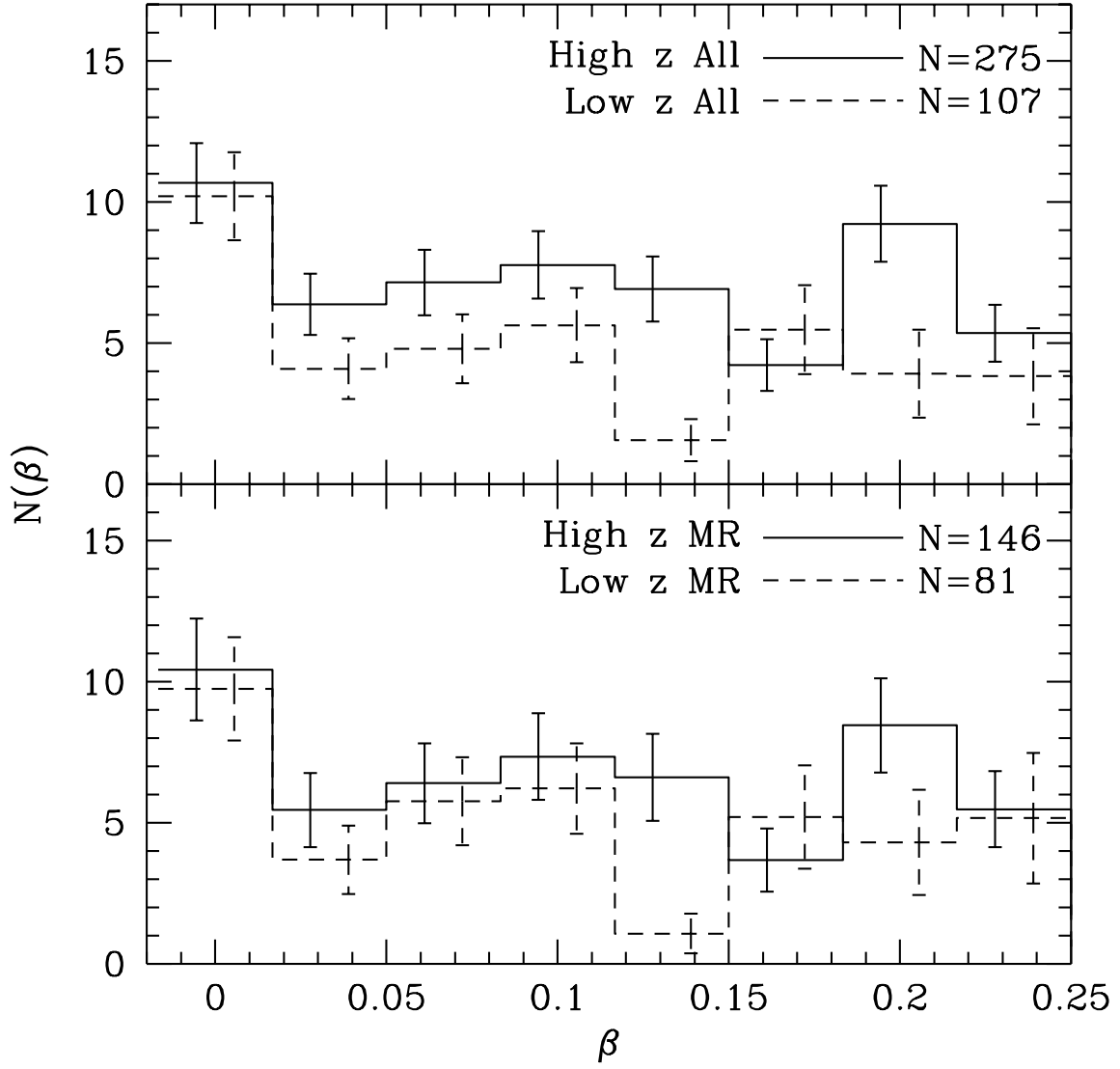


Fig. 3.— Same as for Fig. 1 but for high-redshift and low-redshift QSOs. The absolute visual magnitude (M) and radio luminosity (R) have been normalized in the lower panel.

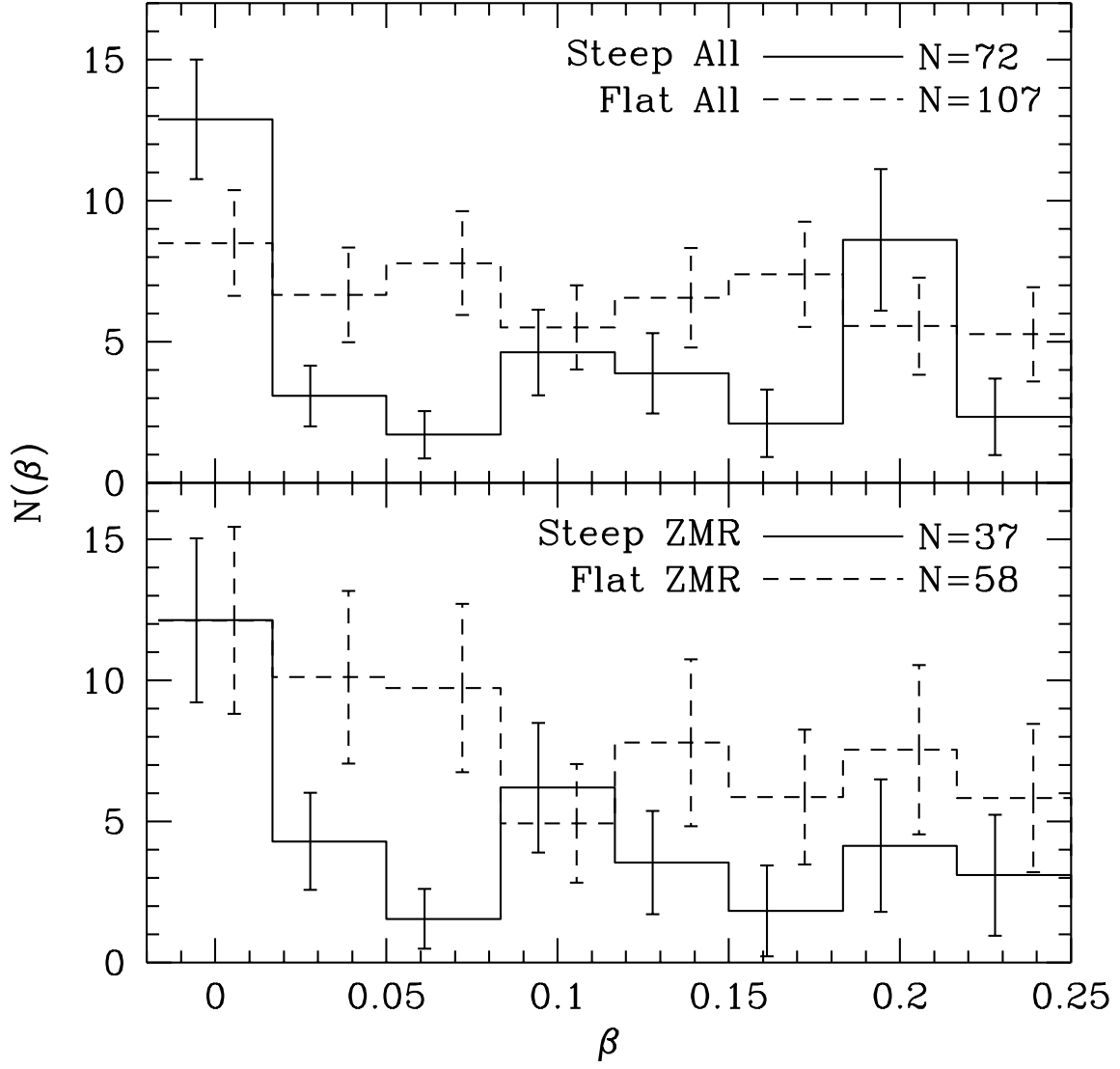


Fig. 4.— Same as for Fig. 1 but for steep-spectrum versus flat-spectrum QSOs. In the lower panel, z_{em} , M_V , and radio luminosity have been normalized for the two samples.

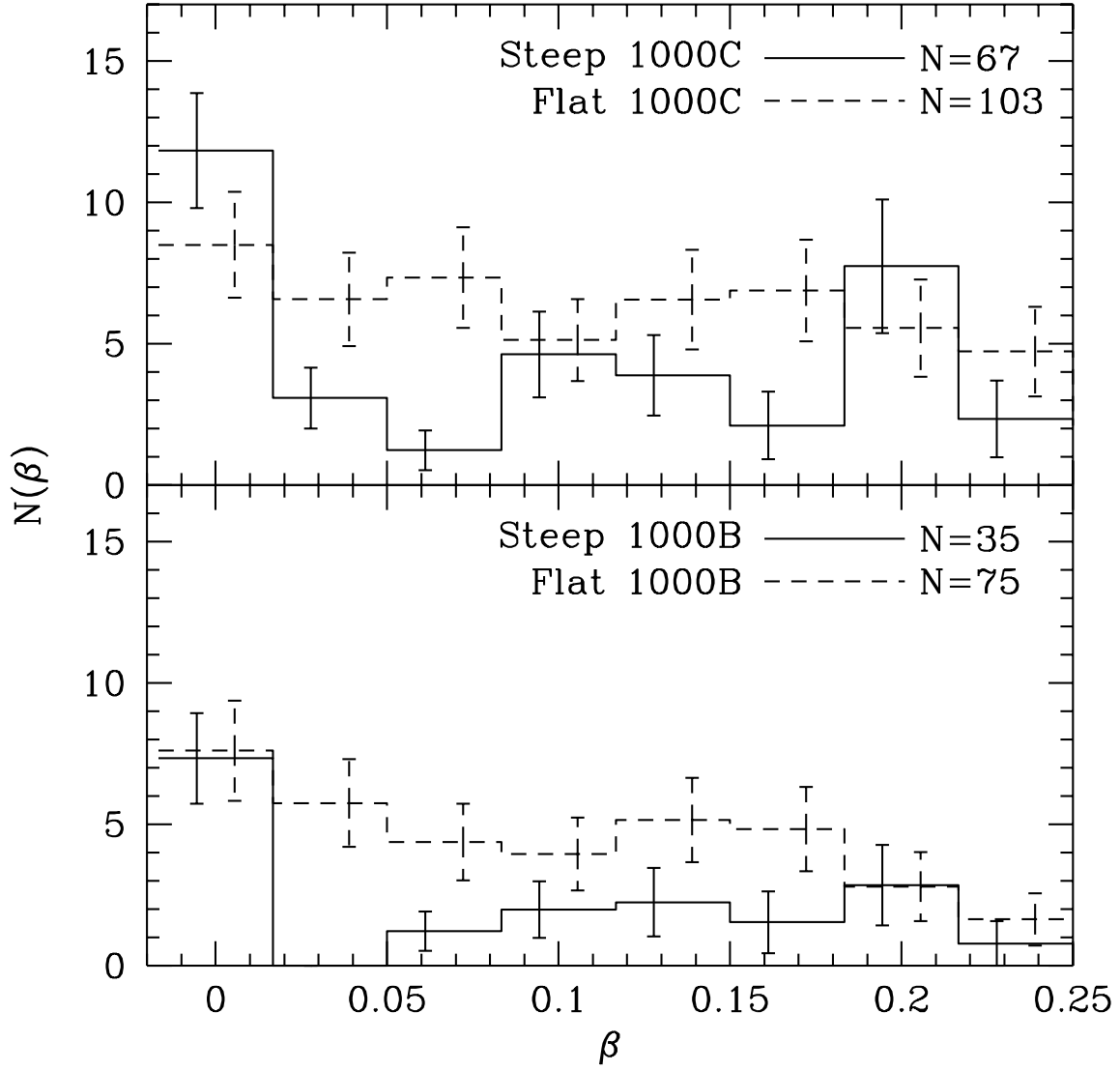


Fig. 5.— Same as Fig. 4 but for A,B, and C graded absorbers combined within 1000 km s^{-1} (*top*) and for A and B graded absorbers combined within 1000 km s^{-1} (*bottom*).

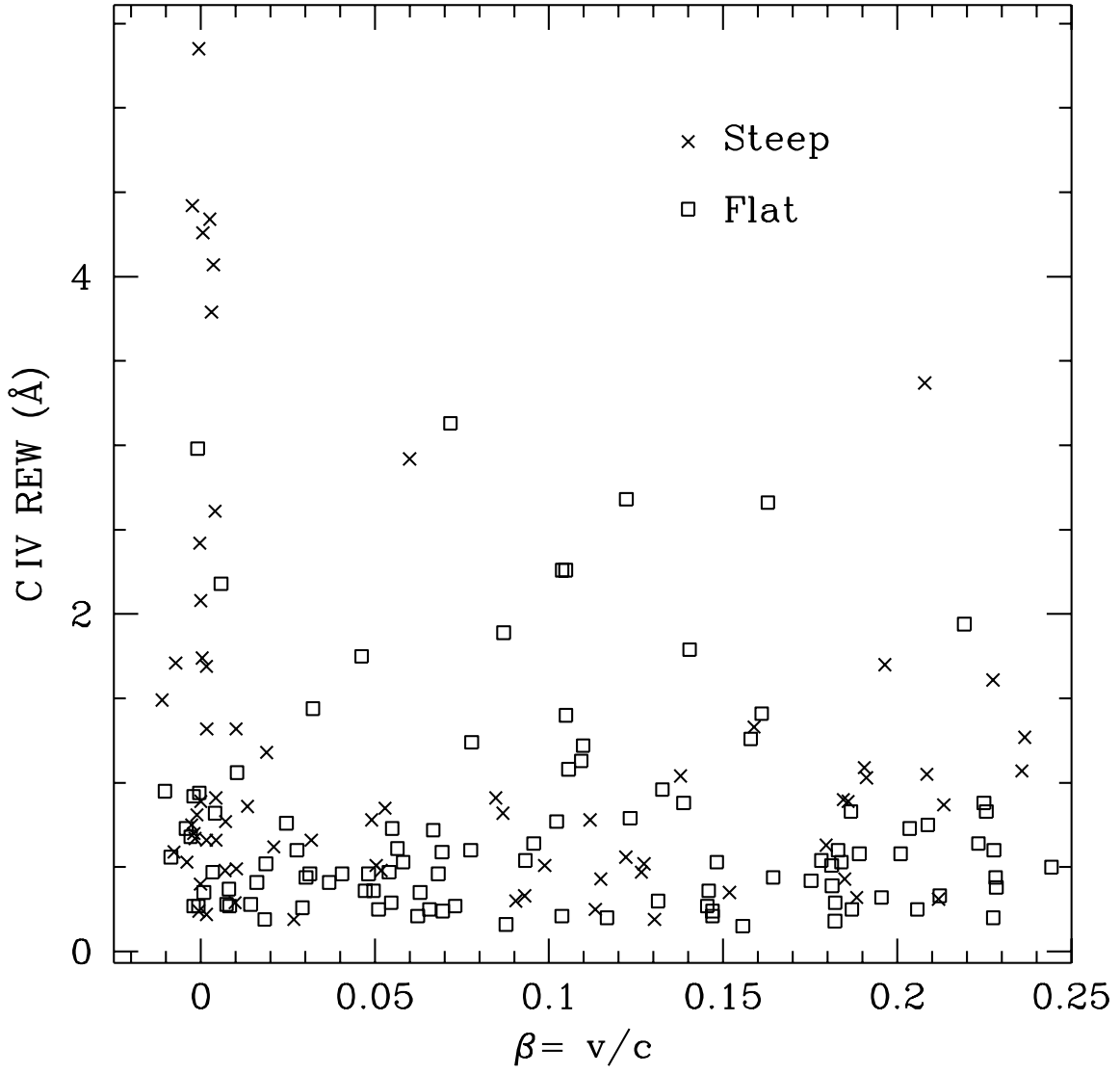


Fig. 6.— Rest Equivalent Width (REW) versus ejection velocity (β) for both flat- and steep-spectrum QSOs. Note the excess of strong absorbers in flat-spectrum QSOs at high velocities.

Relativistic Jet + Beaming Cone

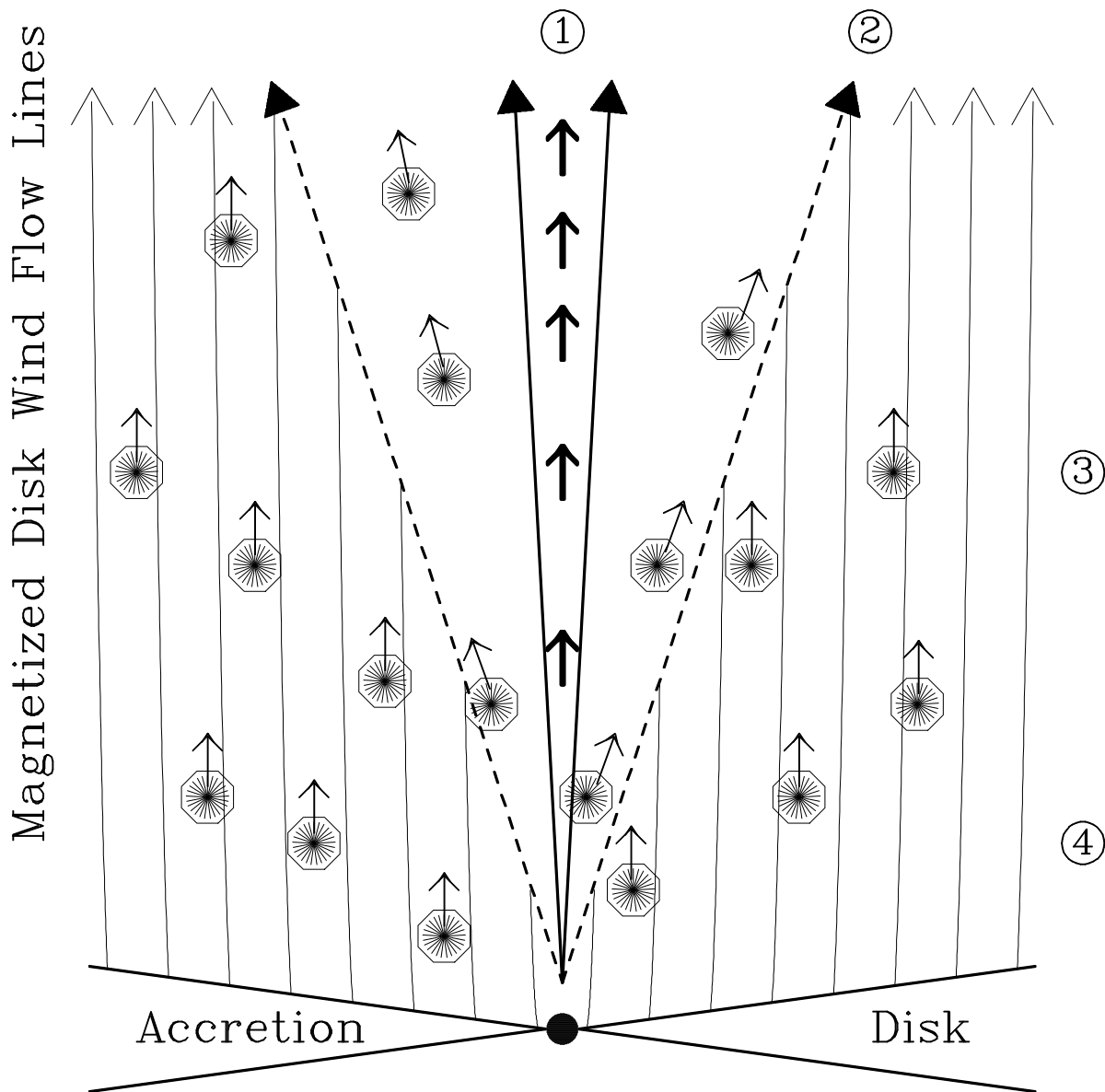


Fig. 7.— Model of the region near the central engine of a QSO. Here the magnetic field lines are perpendicular to the plane of the disk. Sight line 1 represents a BL Lac line of sight. A line of sight through 2 would generally have a flatter radio spectrum than a line of sight through point 3; however, this is not to say that 2 and 3 are lines of sight to flat- and steep-spectrum QSOs, respectively, but rather that steep-spectrum QSOs are generally observed closer to the plane of the disk than flat-spectrum QSOs. If BALs are formed from material stripped off a torus (not shown) in the plane of the accretion disk, then a line of sight through 4 would represent BALQSOs. (Courtesy Arie König and John Kartje)

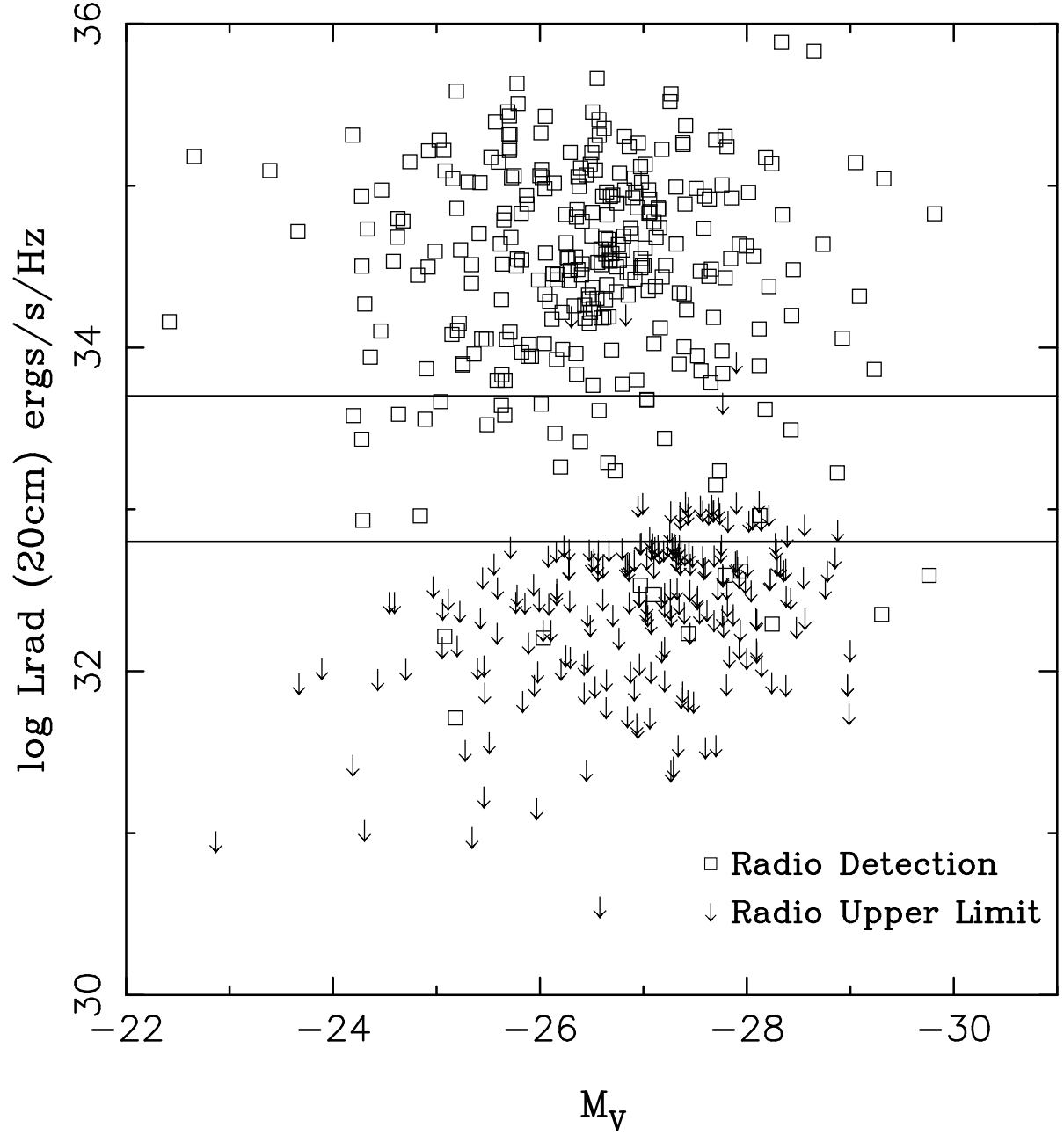


Fig. 8.— 1.4 GHz radio luminosity versus optical absolute magnitude. The two solid lines show the cuts used to determine RL versus RQ.

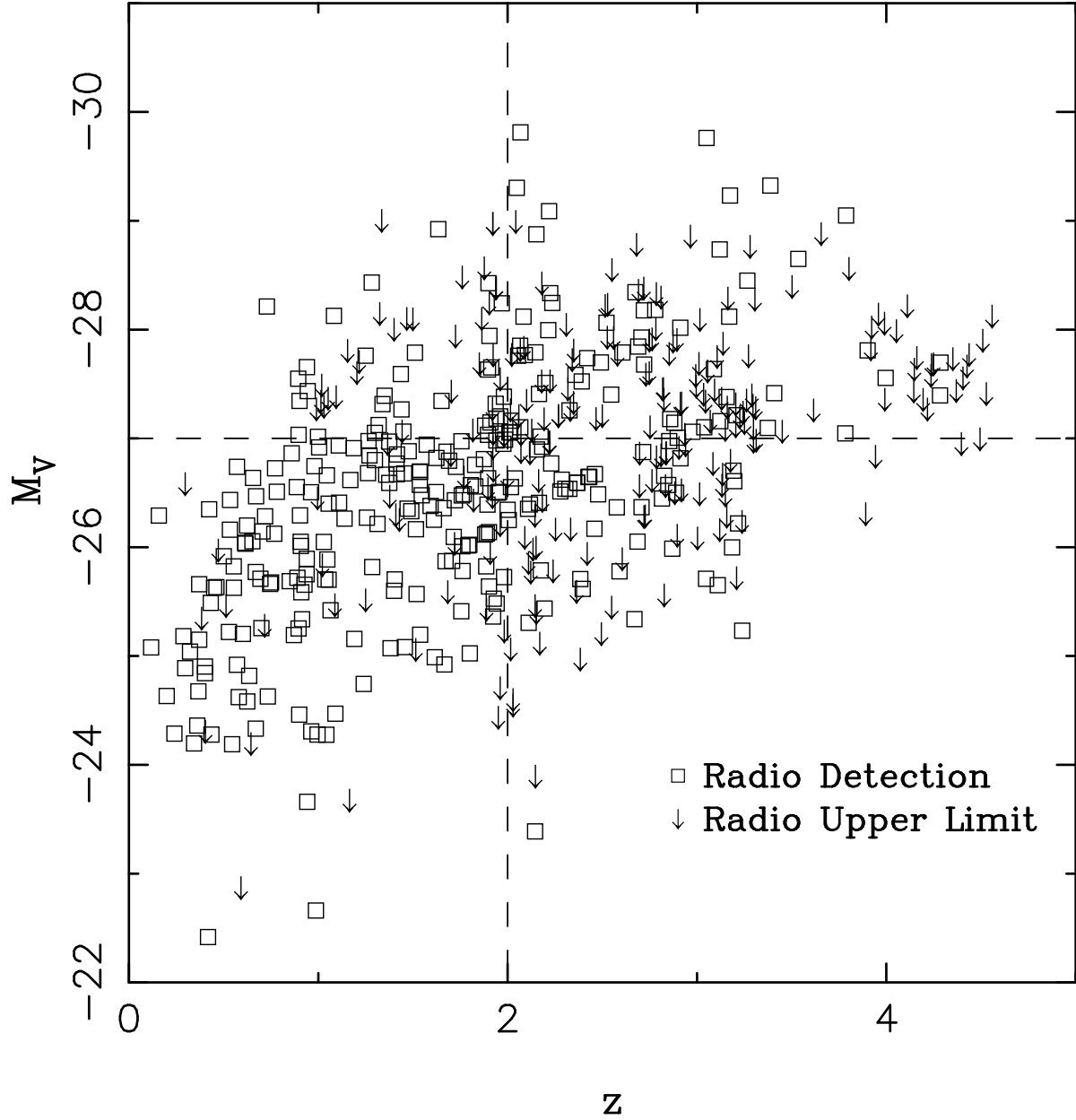


Fig. 9.— Absolute optical magnitude versus redshift. Arrows indicate upper limits to the radio luminosity and are mostly RQ, whereas squares represent detections that are largely RL. Dashed lines indicate the dividing lines between our samples. Note the expected lack of high- z , faint QSOs and bright, low- z QSOs.

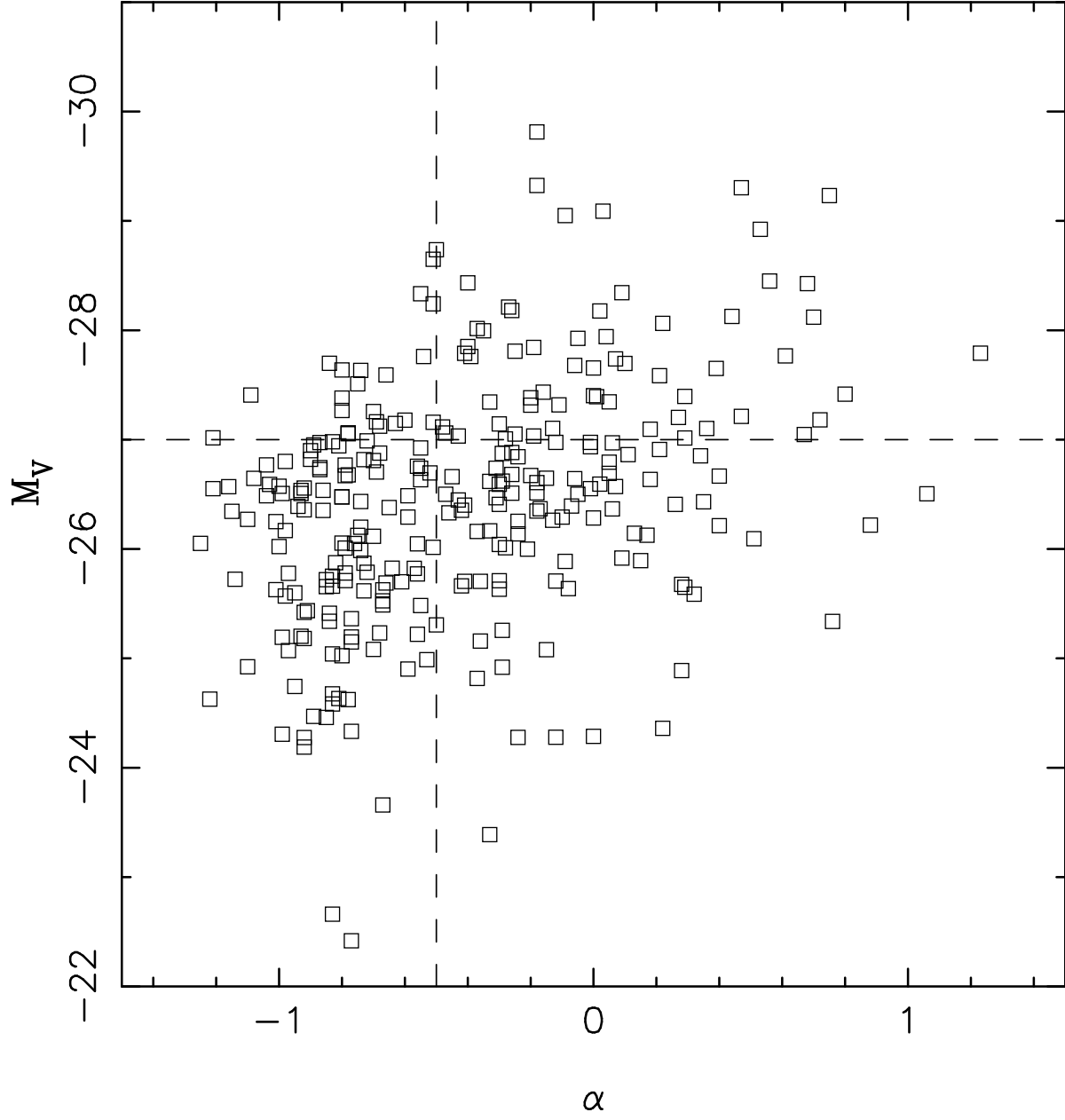


Fig. 10.— Absolute optical magnitude versus radio spectral index. Only radio detections are plotted. Dashed lines indicate the dividing lines between QSO properties in our samples. Note the excess of faint, steep-spectrum objects in the lower left quadrant and the dearth of bright, steep-spectrum objects in the upper left quadrant.

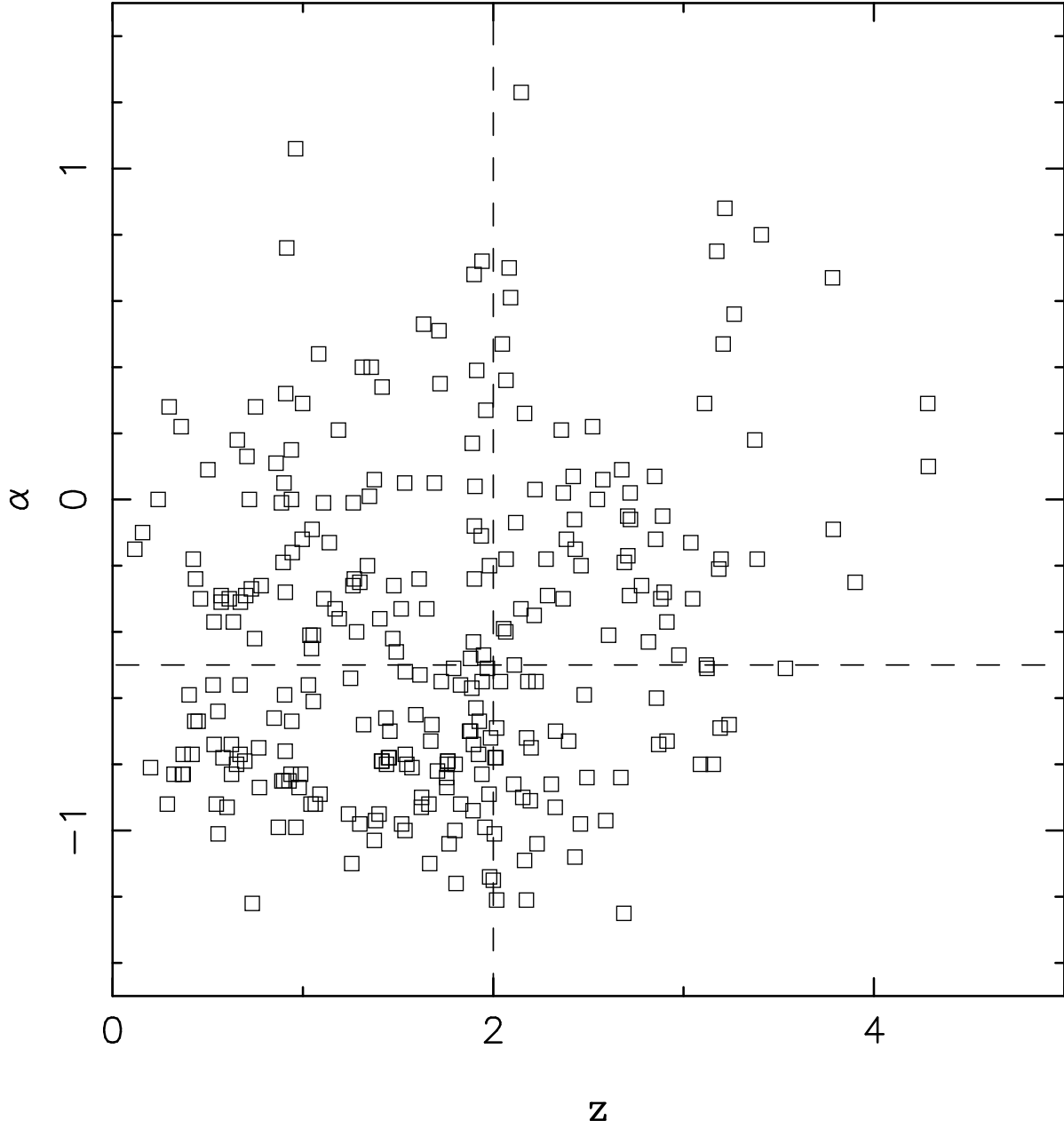


Fig. 11.— Radio spectral index versus redshift. Dashed lines break the plot into two our pairs of samples. Apparent here is the expected lack of high redshift, steep-spectrum objects.

Table 1. Mean $d\mathcal{N}/d\beta$ tests

Sample	5000 km s ⁻¹ to 35,000 km s ⁻¹			5000 km s ⁻¹ to 65,000 km s ⁻¹		
	$\Delta d\mathcal{N}/d\beta$	Std. Dev.	Signif. (σ)	$\Delta d\mathcal{N}/d\beta$	Std. Dev.	Signif. (σ)
Bright/Faint						
250 C	3.236	0.921	3.511	3.143	0.661	4.753
250 C ZR	3.316	1.173	2.828	2.906	0.839	3.464
1000 C	2.694	0.897	3.002	2.828	0.645	4.383
1000 B	1.909	0.697	2.741	1.989	0.495	4.014
Loud/Quiet						
250 C	3.336	1.063	3.137	1.945	0.769	2.530
250 C ZM	4.096	1.343	3.049	2.090	0.937	2.232
1000 C	2.922	1.027	2.845	1.730	0.748	2.315
1000 B	1.536	0.796	1.928	0.803	0.571	1.407
High z/Low z						
250 C	2.254	0.962	2.344	2.697	0.663	4.065
250 C MR	1.174	1.179	0.996	1.947	0.809	2.405
1000 C	2.585	0.918	2.817	2.992	0.635	4.715
1000 B	2.011	0.707	2.844	2.192	0.481	4.558
Steep/Flat						
250 C	3.519	1.176	2.992	2.577	0.909	2.835
250 C ZMR	4.246	1.877	2.262	4.070	1.318	3.089
1000 C	3.369	1.145	2.942	2.562	0.887	2.888
1000 B	3.622	0.896	4.041	2.836	0.680	4.169

Note. — Given are the differences in the mean values of $d\mathcal{N}/d\beta$, the standard deviation of these differences and their significance for four different samples with respect to four sets of QSO properties in two different velocity bins. ZR, ZM, MR, and ZMR refer to properties that have been normalized in a given sample, see Figs. 1– 5 for an explanation of the samples.